VEOLIA-ETH collaboration on

improving Water Stress Index (WSI):

Final report of phase 1

V 1.1

October 3th 2012

Manu Gomez, Stephan Pfister

Contents

1 Introduction

For numerous years now land surface and hydrological models were developed modeling water availability on a global scale with an increased spatial resolution of 0.5° x 0.5°. Until recently, water availability has been studied on a yearly basis only (e.g. Hanasaki et al. (2008a)). However, it has become broadly agreed upon that seasonal and sub-annual availability can differ significantly from the average annual availability. Therefore, it has become state of the art to consider seasonal or monthly variations of water availability (e.g.Flörke and Eisner S. (2011) Voss, Flörke et al. (2009) and Flörke and Alcamo (2004)).

Furthermore, the importance of differentiating between ground- and surface water availability is increasingly emphasized (e.g. CEH Centre for Eclogy & Hydrology (), Wada, van Beek et al. (2010), Döll and Fiedler (2008) and Döll, Hoffmann-Dobrev et al. (2011 (article in press))). Wada, van Beek et al. (2010) as well as Alcamo, Döll et al. (2003) and Döll, Hoffmann-Dobrev et al. (2011 (article in press)) published articles on the modeled data on annual groundwater recharge and groundwater recharge fractions. However, there is still a lack of publications analyzing groundwater and surface water availability on an increased temporal resolution, e.g. monthly values.

2 Water availability

2.1 Literature

It has only been in the context of the *Integrated Project Water and Global Change (WATCH)*, that model output data has been made available with high spatial and temporal resolution for different models (http://www.eu-watch.org). WATCH aims at bringing *"together the hydrological, water resources and climate communities, to analyse, quantify and predict the components of the current and future global water cycles and related water resources states and clarify the overall vulnerability of global water resources related to the main societal and economic sectors*" (EU Sixth Framework Programme 2007-2011).

The WATCH Project comprises eleven hydrological and land surface models (see Table 2). Among others the WaterGAP (Alcamo, Döll et al. 2003), the LPJml (Rost S. 2008), the Joint UK Land Environment Simulator (http://www.jchmr.org/jules) as well as the H08 (Hanasaki, Kanae et al. 2008a) model. Haddeland et al. (2011) compare those models in an excellent overview. Further information on the different models and the project is given in technical reports that can be downloaded from the WATCH Project webpage (www.eu-watch.org/publications). Report No. 34 is particularly recommendable because it outlines recent model improvements. In a multi-model analysis Haddeland et al. (2011) found that *"differences between hydrological model results [...] a major source of uncertainty"* (Haddeland, Clark et al. 2011 : 882). In order to reduce uncertainties, certain parameters were standardized in the context of the WATCH project. These are for instance the following:

- *"Definition of regions*
- *Definition of time periods*
- *Standardized hydro-meteorological input data* (e.g. temperature or precipitation)
- *Standardization of other input data"* (WATCH Technical report No. 1: 4)

With regard to anthropogenic water withdrawal it has to be emphasised that in the WACHT project the models are run under naturalized conditions meaning that anthropogenic water withdrawal and dams are not considered.

Remaining uncertainties can be attributed to the fact that the models are set up very differently. Some solve the energy balance while others do not. Furthermore evapotranspiration as well as the runoff is modelled differently from model to model. Evapotranspiration can for instance be based on the Penman-Monteith, the Priestley-Taylor or a bulk formula. Runoff can be modelled based on infiltration excess using Darcy, on saturation excess (modelling runoff as a nonlinear function of soil moisture) or both (compare Table 1 of Haddeland et al. (2011)). The highest uncertainty is due to different snow water equivalent and soil moisture as well as potential evapotranspiration (Voss, Alcamo et al. 2008: 17)

In the following the WaterGAP, the LPJml, the JULES as well as the H08 model are shortly described.

WaterGAP

A good resume of the modelling approach of the WaterGAP model is given by Flörke et al. (Flörke and Alcamo 2004: 10): *"The aim of the Global Hydrology Model is to simulate the characteristic macro-scale behaviour of the terrestrial water cycle in order to estimate water availability. Herein, water availability is defined as the total river discharge, which is the sum of surface runoff and groundwater recharge. The model covers most of the terrestrial surface of the earth with a geographic grid containing 66896 grid cells with a size of 0.5° by 0.5° (geographical longitude and latitude, respectively) which covers the entire global land area except Antarctica (IMAGE 2.2 land mask). For each grid cell, information on the fraction of land area and of freshwater area (lakes, reservoirs, and wetlands) is available. Land cover is assumed to be homogeneous within each grid cell. The upstream/downstream relationship among the grid cells is defined by a global drainage direction map (DDM30) which indicates the drainage direction of surface water (Döll and Lehner, 2001). Thus, each individual grid cell is assigned to a drainage basin. The model calculates a daily vertical water balance for each grid cell, separately for the fraction of land area and for the freshwater area. The vertical water balance of land areas is described by a canopy water balance (representing interception) and a soil water balance. The canopy water balance determines which part of the precipitation is intercepted (evaporates) by the canopy, and which part reaches the soil. The model balances incoming precipitation with actual evapotranspiration and total runoff. Then, the total runoff from land area is divided into surface runoff and groundwater recharge, using information on cell-specific slope characteristics, soil texture, hydrogeology, and the existence of permafrost and glaciers. Aside from calculating the land area water balance, a vertical water balance for the freshwater areas (lakes, reservoirs, and wetlands) is calculated. The runoff from open freshwater bodies is defined as the difference between effective precipitation and potential evaporation. Finally, the total runoff of a grid cell is the sum of the runoff from land and from open freshwater bodies. In the model, it is distinguished between 'local' and 'global' open freshwater bodies. In contrast to the local lakes and wetlands, which only consider flow-through processes within a cell, global open freshwater bodies are additionally flowed through from neighbouring cells. The runoff produced within the cell and the volume of water coming from upstream cells is transported through a series of storages representing the groundwater, lakes, reservoirs, wetlands, and rivers. Then, the total cell discharge is routed along the drainage direction map (DDM30) to the next downstream cell. The hydrological model requires data about precipitation, potential evapotranspiration, and temperature for each grid cell. As climate input, the data by New et al. (2000) provide observed monthly values of precipitation, temperature, number of wet days, average daily sunshine hours, cloudiness, and global radiation, interpolated onto a 0.5° by 0.5° grid and for each of the years 1901 to 1995. In the Global Hydrology Model, the calculations are performed on a daily resolution. Synthetic daily precipitation values are generated using monthly precipitation values and the number of wet days per month, the monthly precipitation is distributed equally to all rainy*

days. In order to take into account the effect of snow, effective precipitation, which is the sum of precipitation as rainfall and snowmelt, is calculated using a degree-day algorithm. Future climate is simulated by changing the monthly temperature and precipitation observed in the so-called climate normal period (1961-1990) according to future climate projections from general circulation models (GCMs). The Global Hydrology Model is calibrated against long-term average annual discharges measured at 724 gauging stations world-wide, the drainage areas of which cover half the global land area except Greenland and Antarctica. In Europe, the model has been calibrated in 126 drainage basins, covering 65% of Europe's land area (Lehner et al., 2001)."

A corresponding short version is given in the WATCH Technical Report No. 1 (Voss, Alcamo et al. 2008: 7): *"WaterGAP comprises two main components, a Global Hydrology Model and a Global Water Use Model. The Global Hydrology Model simulates the macroscale behaviour of the terrestrial water cycle to estimate water resources, while the Global Water Use Model computes water use for the domestic, industrial, irrigation and livestock sectors. Both water availability and water use computations cover the entire land surface of the globe (except the Antarctic) and are performed for cells on a 0.5° by 0.5° spatial resolution. The WaterGAP-Global Hydrology Model calculates a daily vertical water balance for both land area and open water bodies in each 0.5-cell. The sum of runoff produced within a cell plus the upstream discharge into a cell is transported through groundwater, lakes, reservoirs and wetlands to rivers. Finally, the river discharge is routed to the next downstream cell according to a global drainage direction map (Döll & Lehner 2002). The calculated total discharge has been calibrated against measured values (from GRDC, 2000) for 724 drainage basins worldwide. The calibration procedure is implemented via tuning of a model parameter describing the land surface runoff to achieve a sufficient match to observed longterm average annual discharge. For drainage basins without measured discharge data, runoff factors are regionalized by applying a multiple regression approach (Döll et al., 2003)."*

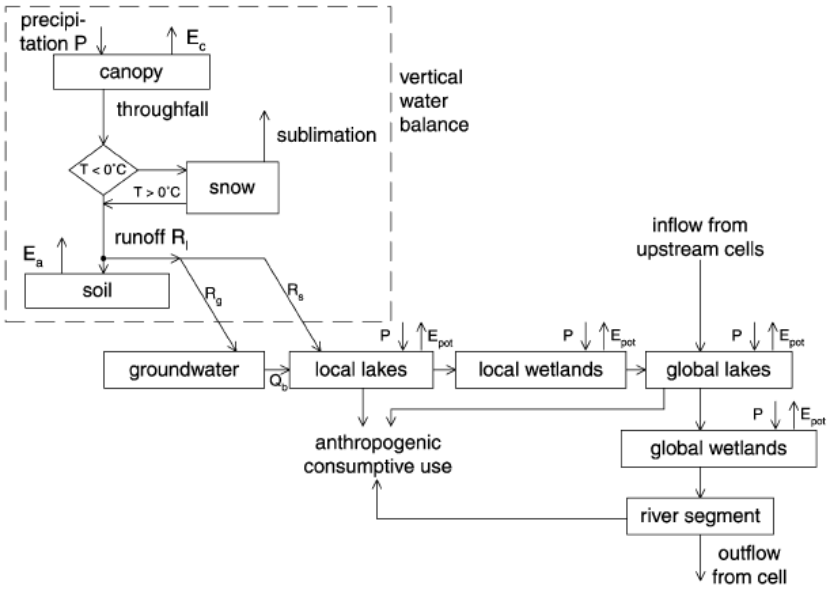

Figure 1: "Schematic representation of the global hydrological model WGHM, a module of WaterGAP 2" (Döll, Kaspar et al. 2003)

LPJml

The Lund-Potsdam-Jena managed Land model (LPJml) is a *"dynamic global vegetation and water balance model"* (Rost S. 2008: 2). It *"computes the establishment, growth and productivity of the world's major natural and agricultural plant types and the associated carbon and water fluxes as*

well as their spatiotemporal variations in response to climatic conditions and human interferences such as irrigation, typically on a 05° grid and at daily time step. […] As LPJml simulates the terrestrial water balance realistically and in coupling with the dynamics of natural and agricultural vegetation, it is well suited of assessing global green and blue water fluxes, and their inter-annual variations, in a consistent and process-based manner" (Rost S. 2008: 2).

"The LPJmL model simulates key ecosystem processes such as photosynthesis, evapotranspiration, autotrophic and heterotrophic respiration, as well as allocation of assimilated carbon to different above- and below-ground pools. It considers nine natural plant functional types (PFTs) and twelve crop functional types (CFTs), which correspond to the world's most important field crops (temperate cereals, temperate roots, tropical cereals, tropical roots, rice, maize, pulses, sunflower, soybean, groundnuts, rapeseed) and pasture (grazing land). Carbon fluxes and vegetation dynamics are directly coupled to water fluxes in the model, in that, e.g., photosynthesis and transpiration are treated as simultaneous processes [Sitch et al., 2003; Gerten et al., 2004b]. [41] The PFTs can coexist in any grid cell, but their abundance depends on competition for light, water (e.g., through distribution of fine roots) and space as well as on environmental (e.g., bioclimatic) constraints. This way, the distribution, fractional coverage and seasonal phenology of PFTs change depending on climate, water availability, and disturbances such as fire. A grid cell can contain several stands differentiated between rainfed and irrigated CFTs and one stand for PFTs. Each stand in a grid cell shares the same climate input, but the water balance is computed separately." (Rost S. 2008: 12)

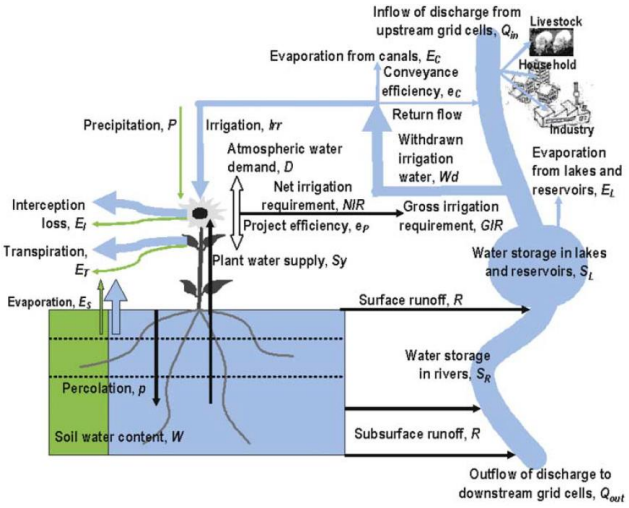

Figure 2: "Schematic representation of green and blue water flows as computed in the LPJmL model" (Rost S. 2008)

Jules

Information and good explanations on the modelling approach behind the Joint UK Land Environment Simulator (JULES) can be withdrawn from http://www.jchmr.org/jules.

"The Joint UK Land Environment Simulator (JULES) is a process-based model that simulates the fluxes of carbon, water, energy and momentum between the land surface and the atmosphere." (Clark, Mercado et al. 2011: 701). The model is a further development of the land surface scheme Mat Office Surface Exchange Scheme (Moses) and the dynamic global vegetation model TRIFFID (Clark, Mercado et al. 2011) described by Cox et al. (1999) and Essery et al. (2003). *"MOSES was originally designed to represent the land surface in Meteorological and Climate models, but is increasingly used for other purposes: predicting river flows, identifying global wetlands, quantifying water resources. It was therefore decided to officially release the model from its original role in two ways. Firstly, the model should become a community model and secondly, the model should be used and developed independently of the meteorological and climate model."* (Met Office and CEH

Centre for Eclogy & Hydrology 2011). *"The model hydrology is described in (Gregory, Smith et al. 1994).*

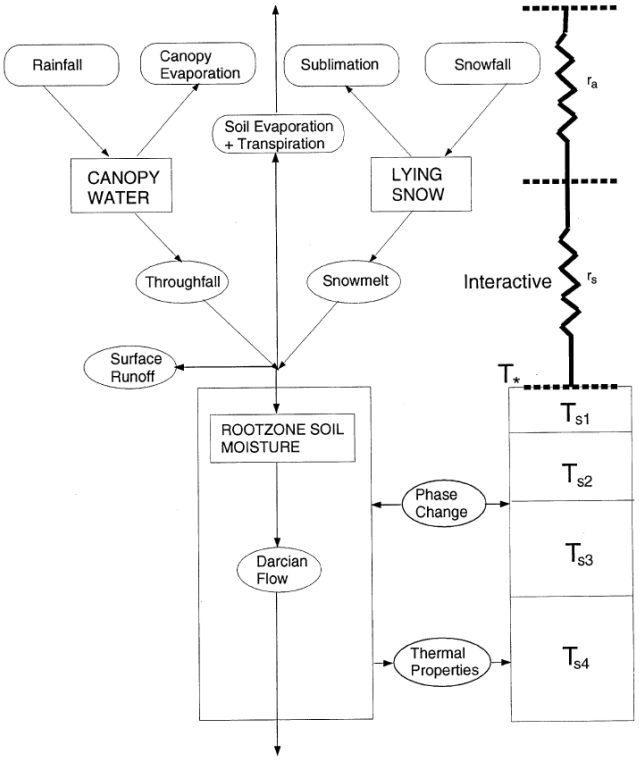

Figure 3: "Schematic representation of the Meteorological Office surface exchange scheme (MOSES)" (Cox, Betts et al. 1999) on which the JULES model is based on.

H08

"The [H08] *model consists of six modules: land surface hydrology, river routing, crop growth, reservoir operation, environmental flow requirements estimate, and anthropogenic water withdrawal. It simulates both natural and anthropogenic water flow globally on a daily basis.* […] *with water and energy balance closure. The crop growth module of H08 estimates planting and harvesting dates globally, and the land surface hydrology module calculates daily evapotranspiration from cropland during cropping periods. Since rain fed cropland and irrigated cropland have independent soil moisture in each grid cell, evapotranspiration is calculated separately. […] The river routing module simulates daily streamflow. The 452 largest reservoirs worldwide that have greater than 10^9 m^3 storage capacity (hereafter, large reservoirs) are individually geo-referenced to the digital river map of the H08 model (Hanasaki, Kanae et al. 2006) and their operations influence the streamflow simulation. The original H08 model limits the water withdrawal source to streamflow. The allocated environmental flow requirement is always left in the channel. […] The land surface hydrology module of H08 deals with the upper soil layer (0–1 m) and separates precipitation into evapotranspiration and runoff. Therefore, shallow groundwater recharge is included in runoff. However, deep groundwater, lakes, and glaciers are not modelled in the H08 model because they formed over decades and centuries and are beyond the time frame of the H08 simulation. Water diversion and desalinization are also not modelled because these activities transport fresh water beyond grid cells.* (Hanasaki, Inuzuka et al. 2010: 233)

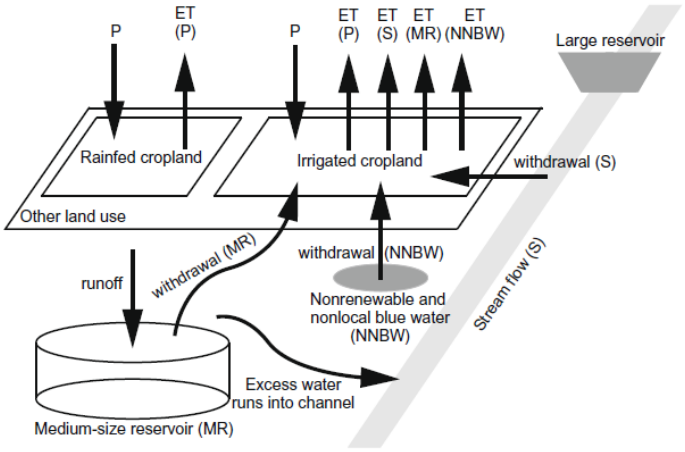

Fig. 2. Schematic diagram of water withdrawals in the H08 model.

Figure 4: ***"Schematic diagram of water withdrawal in the H08 model"*** **(Hanasaki, Inuzuka et al. 2010: 235)**

Table 1 gives an overview of the main characteristics of the different models (hydrological model component only).

Table 1: Comparison of main hydrological model characteristics (WATCH Technical Report 56)

Model Type	**Model Name**	Model time step	Meteorological forcing variables†	Energy balance	Evapotranspiration scheme	Runoff scheme††	Snow scheme
Global hydrological models	**WaterGAP**	Daily	P, T, LWn, SW	No	Priestley-Taylor	Beta function	Degree day
	LPJmL	Daily	P, T, LWn, SW	No	Priestley-Taylor	Saturation excess	Degree day
Land surface models	**JULES**	Hourly	R, S, T, W, Q, LW, SW, SP	Yes	Penman-Monteith	Infiltration excess/ Darcy	Energy balance
	H08	Daily	R, S, T, W, Q, LW, SW, SP	Yes	Bulk Formula	Saturation excess/ Beta function	Energy balance

† R: rainfall, S: snowfall, P: precipitation, T: mean daily air temperature, W: wind speed, Q: specific humidity, LW: longwave radiation flux (downward), LWn: net longwave radiation, SW: short wave radiation, SP: surface pressure
†† Beat function: Runoff is a nonlinear function of soil moisture

2.2 Data processing

In the WATCH project the data is provided in the netCDF data format with one .nc file for each year. An overview of the models and the data provided for discharge and subsurface runoff (as explained later) is given in Table 2. The models that do not provide discharge results are eliminated from our analysis (CLM-EHT, GWAVA, Htessel, MacPDM and VIC). For the remaining models (H08, Jules, LPJ, Matsiro MPI-HM, Orchidee and WaterGAP) data was downloaded from the CEH Information Gateway (CEH Centre for Eclogy & Hydrology) as described in Table 3.

Table 2: Overview of the model output data, available on the CEH Information Gateway. The values indicate the available time period for the corresponding model and variable.

Model name	Discharge (Dis) [m^3/s]	Subsurface runoff (Qsb) [mm/s]
GWAVA	No	1971-2000
H08	1963-2001	1963-2001
Htessel	No	1963-2001
Jules	1963-2001	1963-2001
LPJ	1963-2001	1963-2001
MATSIRO	1963-2001	1963-2001
MPI-HM	1963-2001	1963-2001
MacPDM	No	1963-2001
Orchidee (cwrr nat)	1963-2001	1963-2001
VIC	No	No
WaterGAP	1963-2001	1963-2001

Table 3: Accessing WATCH data on the CEH Information Gateway.

WATCH data can be accessed free of charge from https://gateway.ceh.ac.uk/ (registration required). Upon login select “Start Searching” and enter "Watch 20th Century Ensemble Data". Open the corresponding dataset and select the tab "Access" followed by the FTP site.

On that site there is an ensemble product for the seven models at the global scale. This aggregated data can be found in Workblock 1 under 20th Century Ensemble Product. However, only few parameters are available (e.g. the sum of the surface and the subsurface runoff but not the individual values). This ensemble product is described in the Technical Report 37 (Weedon 2011) (http://www.eu-watch.org/publications/technical-reports/2).

The daily discharge data downloaded from the CEH Information Gateway from 1963 until 2001 is aggregated in Matlab first to a daily average per pixel for each day of the year (across all years) and second from pixel to watershed level. For each of the models there is a Matlab file that imports the corresponding netCDF file. Figure 5 summarizes what the Matlab code does. The key output is the monthly discharge per watershed given in m^3/s.

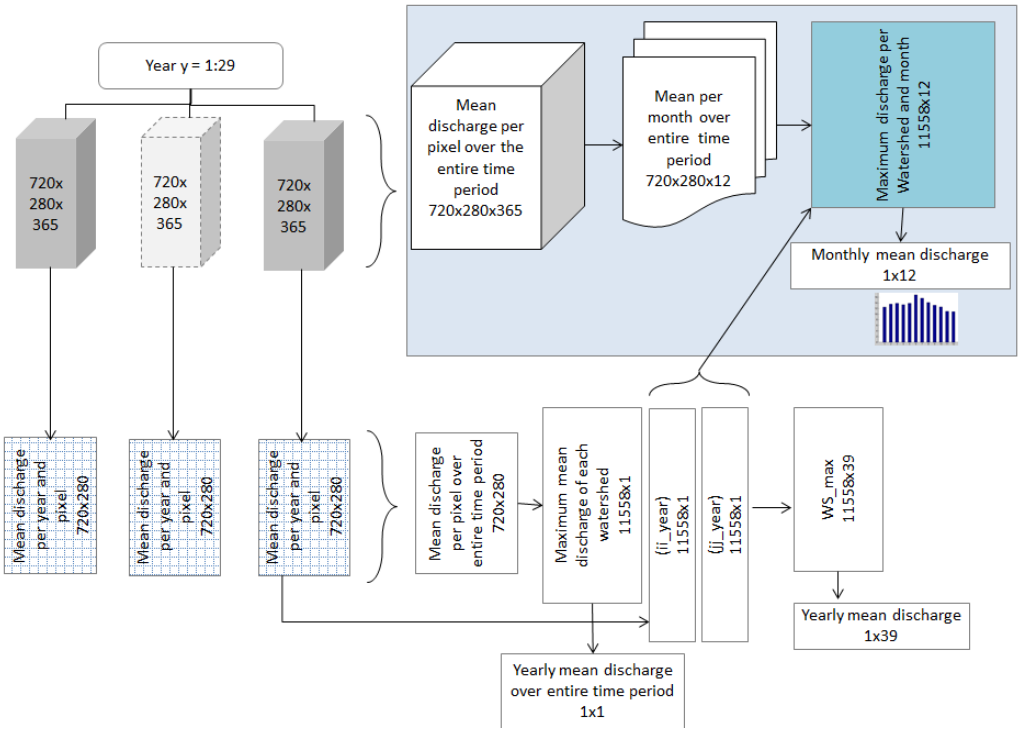

Figure 5: Explanation of the Matlab code that imports the netCDF data, selects for each watershed the cell with the maximum yearly average discharge and gets the monthly average discharge for these cells. The output we are interested in is indicated in blue.

Analysing the WaterGAP data across the entire time period (1963-2001) shows no tendency in the yearly global discharge (see Figure 6). For consistency reasons, all leap years are left out leaving us with the analysis of the 29 non-leap years between 1963 and 2001.

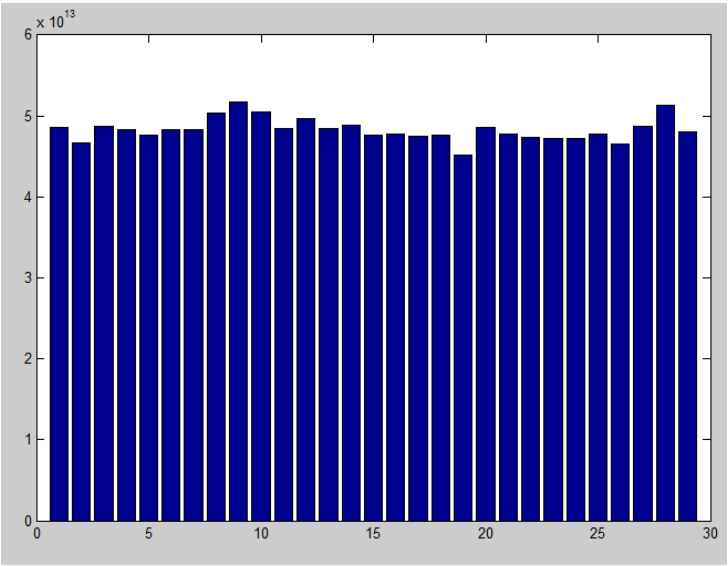

Figure 6: Yearly global discharge [m³/year] modelled with the WaterGAP model. On the x-axis the value 1 represents the year 1963 and the year 29 stands for the year 2001. Leap-years are not considered.

Definition of watersheds

One file in which watersheds are defined is the one called "current_watergap21". That one was used by Stephan for the current WSI. The largest watersheds are split up to a sub-watershed level. We use the watersheds as they were sent to Stephan by Floecke et al. These are apparently the most recent definitions of watersheds. A disadvantage is that the large watersheds are not split up as they were in the old version used.

The file we used is called *"indicator_2010.shp"*. That file is opened in Arcmap and converted to 0.5x0.5 degree grid cells (pixels). The row called "GBASIN" attributed to each of the watersheds a unique value between 1 and 11558. This layer was converted from a raster file to an ascii. (ncol 720, nrows 280, xcorner -180, ycorner -56). Even though the large watersheds are not split up into smaller watersheds there are more watersheds than in the other definition of watersheds. This is largely due to the fact that close to the cost there are more additional watersheds.

Using the same code for seven models (H08, Jules, LPJ, Matsiro MPI-HM, Orchidee and WaterGAP) led to a similar annual mean global discharge for the five models listen in Table 4.

Table 4: Annual mean global discharge for the five models for the time period 1963 to 2001. The results of the different models are in the same order of magnitude.

Model name	Global discharge [E+13 m3/y]
WaterGAP	4.8
JULES	5.3
H08	5.6
MPI-HM	3.3
LPJmL	6.2

The Matsiro model leads to the right order of magnitude but the analysis of individual years does not show any yearly variation. This raises doubts of whether or not the model results are correctly uploaded. Furthermore, when doing the calculations over the entire time period (1963-2001), Matlab runs out of memory. For the Orchidee model the resulting yearly discharge using the exact same Matlab code as for the other models amounts to 2.5E+31 m^3/years which is implausible. For this reasons the Matsiro and the Orchidee model are not further included in the development of the new Water Stress Index. Also the MPI-HM model is eliminated as it leads to a global yearly discharge clearly below the other four models.

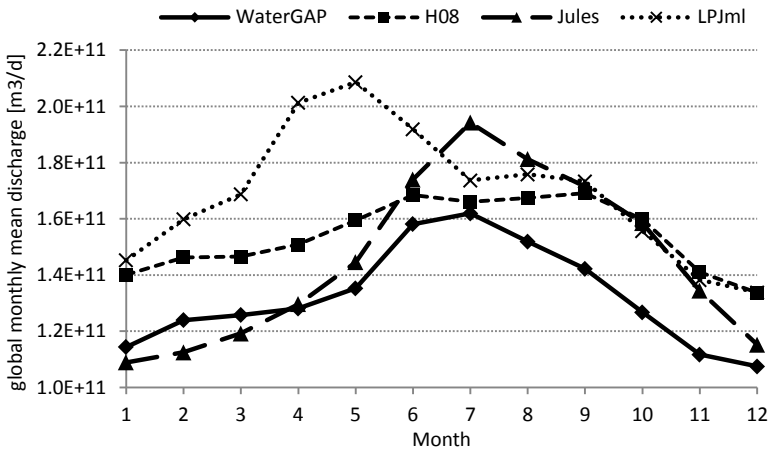

Figure 7: Global monthly discharge for the time period from 1963 to 2001 for the four different models.

The figure below visualizes the yearly discharge [m3/year] on a watershed level for the WaterGAP, the H08, the Jules and the LPJml model (clockwise starting from top left).

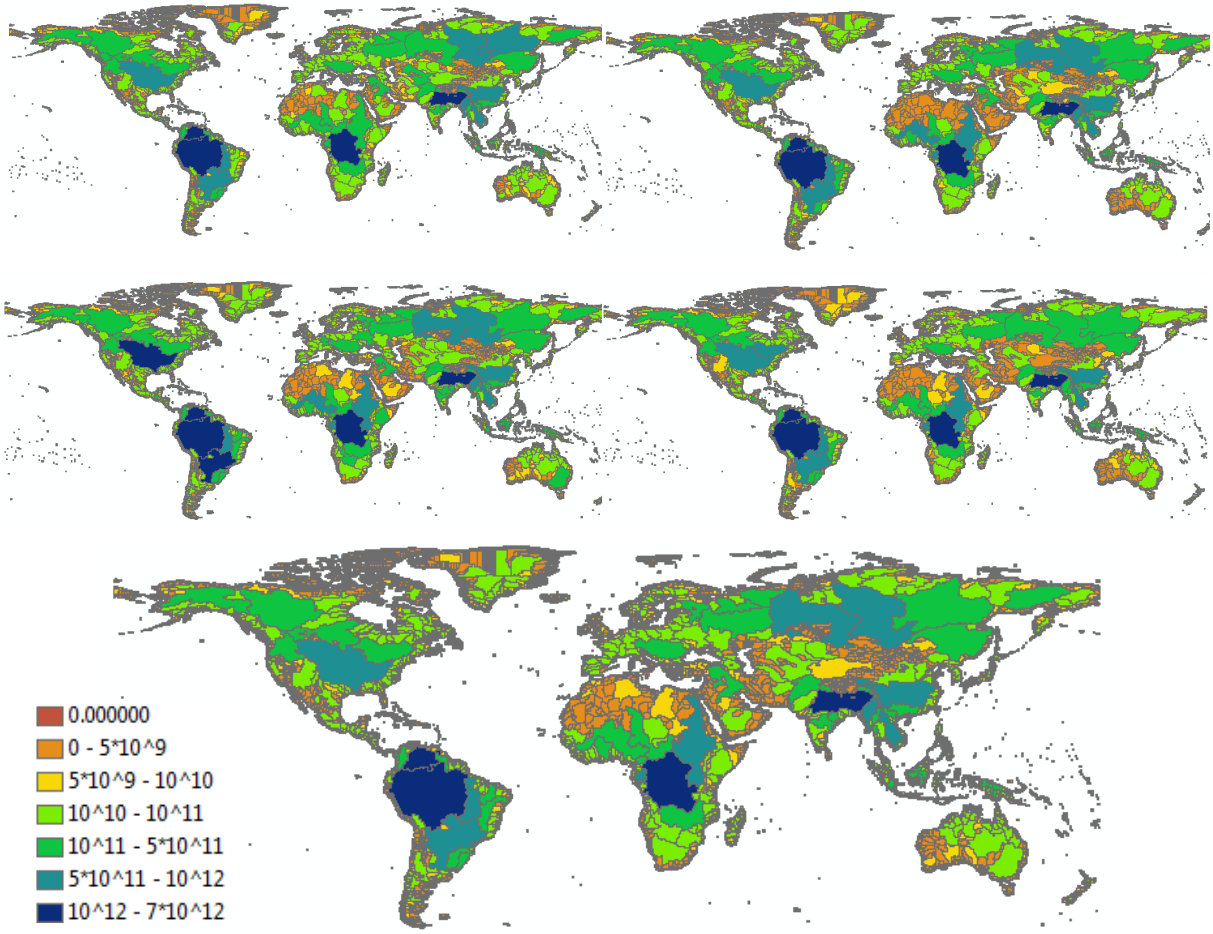

Figure 8: Yearly river discharge [m³/year] on a watershed level for the WaterGAP, the H08, the Jules and the LPJml model (clockwise starting from top left) as well as the average of the four (bottom).

As a measure for the sub-annual variations of water availability on watershed level, the percentage of the difference between the average monthly and the average yearly discharge to the total yearly discharge is calculated as follows:

$$\frac{\sum_{i=1}^{m}(nr\_days_i * |dailyDis_i - dailyDis_{year}|)}{365 * dailyDis_{year}} \cdot 100 \quad (1)$$

Where m is the number of months, nr_days_i is the number of days in the respective month, $dailyDis_i$ is the discharge on an average day in the respective month and $dailyDis_{year}$ is the discharge on an average day considering the entire year.

Figure 9 depicts for each watershed the percentage obtained with Equation (1. It becomes clear that water availability shows significant sub-annual variations especially in arid and semi-arid regions. This variability may lead to increased water scarcity during specific periods, if insufficient water storage capacities are available. In Europe (except southern Europe) and Canada the sub-annual variations are minor.

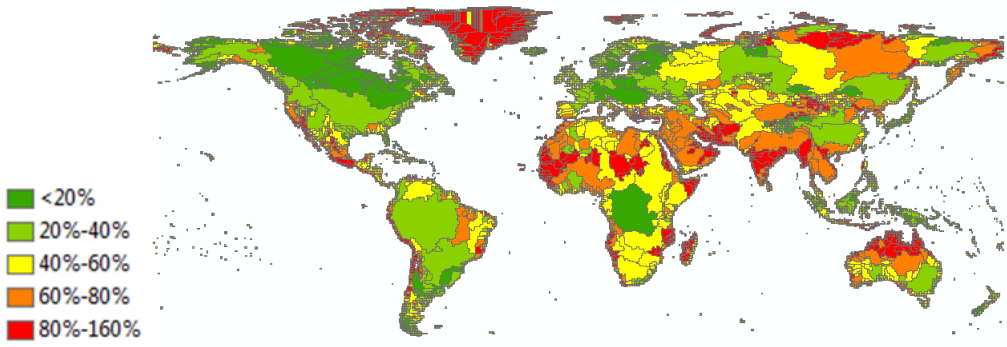

Figure 9: Percentage obtained with Equation (1. The ratio of the difference between the average monthly and the average yearly discharge to the total yearly discharge.

Figure 10 plots the monthly discharge as an example for the Mississippi, the Nile and the Amazon watershed. The simulated monthly flow pattern for the Mississippi agrees with the observed one. Highest flow rates are observed in spring when snow melts and spring rains abound and are lowest in fall.

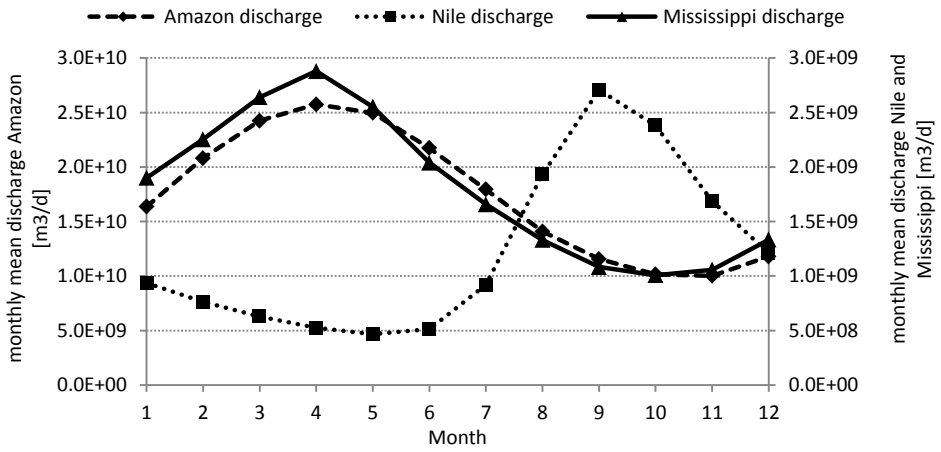

Figure 10: Monthly discharge according to the WaterGAP model in the Mississippi, the Nile and the Amazon watershed.

3 Sectoral water withdrawal and consumption

3.1 Literature

As mentioned above the WaterGAP model consists of a hydrological and a socio-economical part. The latter quantifies the freshwater withdrawal and consumption for different users (Alcamo, Döll et al. 2003). The water withdrawal depicts the total amount of water used in each sector, while the consumption depicts the part of withdrawn water that is evapotranspired, consumed by humans or industrial products. The In the context of the WATCH project these data on sectoral water use has been made available on CEH Information Gateway. Consumption and withdrawal data is given for the irrigation, domestic, electricity production and manufacturing sector. For livestock it is assumed that all the water that is withdrawn is consumed. The data is described in the WATCH Technical Report No. 46 on sectoral water use (Flörke and Eisner S. 2011) as well as the WATCH Technical Report No. 17 (Voss, Flörke et al. 2009). The modelling is done as described by Alcamo et al. (2003) in the context of the WaterGAP Global Water Use model.

The basic approach for estimating the domestic, manufacturing and industry sector is to compute the water intensity and multiply it with the sectoral driving force (population, gross value and electricity production respectively). Two main concepts are used for modelling the change in water intensity: structural change and technological change. These concepts allow a model parameterization using income (GDP/capita) as proxy data. The relationship between water use intensity and income is derived by fitting the structural curve to historical data from each country. The country-level withdrawals are allocated to different grid cells based on the population density, the ratio of rural to urban population and the percentage of population with access to safe drinking water. The irrigation model simulates the cropping pattern, the growing season and the irrigation requirements (withdrawal and consumption) distinguishing two crop types (rice and other crops) for the irrigated areas. The water consumption for irrigation is computed for each day of the growing season as the difference between the potential evapotranspiration and the plant-available precipitation. The required water withdrawal is calculated by considering regionally varying irrigation efficiencies. Table 5 lists the main forcing variables of the water use model for the different sectors.

Table 5: Forcing variables of the water use model for the different sectors (Alcamo, Döll et al. 2003)

Sectoral water use model	Forcing variables
irrigation	Crop type, cropping pattern, irrigated land, climate data, improvement in efficiency
livestock	Number and type of livestock, consumption per head
domestic	Population, GDP per capita, improvement in efficiency
manufacturing	Gross value, improvement in efficiency
electricity	Electricity production, improvement in efficiency

The water withdrawal and consumption data for agricultural irrigation is given as monthly value in the unit mm/month for the time period from 1906 to 2000 with a spatial resolution of 0.5° x 0.5°. The water use data for the other sectors is given as annual value in the units of mm/s for the time period from 1900 to 2000 with a spatial resolution of 0.5° x 0.5°. We use the data given for the year 2000 because this is the most recent data available.

Figure 11 to Figure 16 visualize the WATCH water consumption and withdrawal data for irrigation, livestock, domestic purposes, manufacturing and for electricity generation. The unit mm/year remains the same for all figures. Highest water withdrawals are found in India, eastern China, Europe, Egypt (in the Nile delta) and in the USE at the east and west coast and the higher

Mississippi basin. In Europe, eastern USA the water withdrawal is dominated by the electricity production while agricultural withdrawal is the dominant water use sector in central and western USA, Asia, Africa and China.

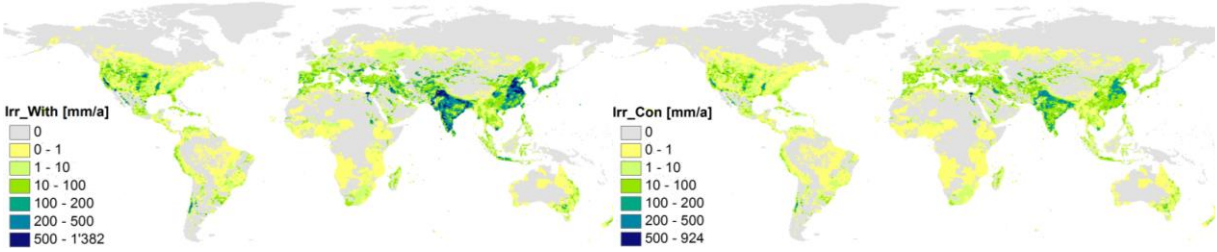

Figure 11: Annual water withdrawal (top) and consumption (bottom) for irrigation in mm/year for the year 2000. Spatial resolution of 0.5° x 0.5°. (CEH Information gateway).

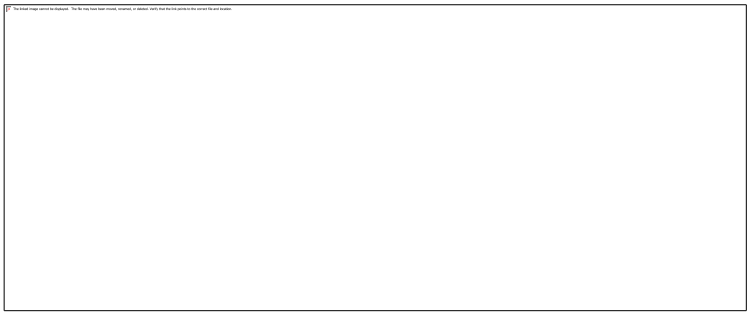

Figure 12: Livestock water consumption (assuming that consumption equals withdrawal) in mm/year for the year 2000. Spatial resolution of 0.5° x 0.5°. (CEH Information gateway).

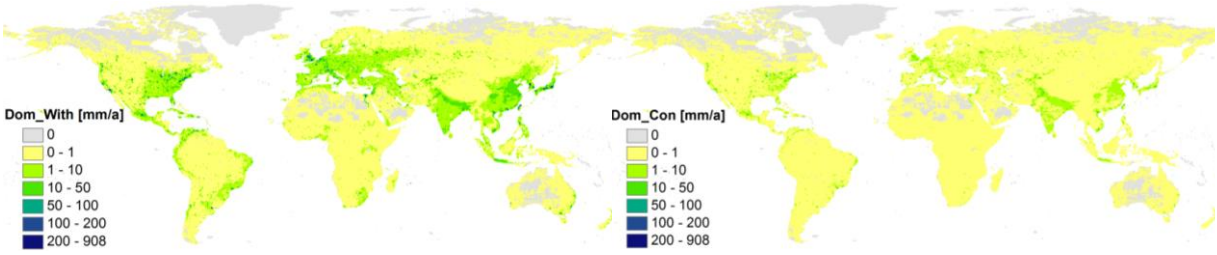

Figure 13: Water withdrawal (top) and consumption (bottom) for domestic purpose in mm/year for the year 2000. Spatial resolution of 0.5° x 0.5°. (CEH Information gateway).

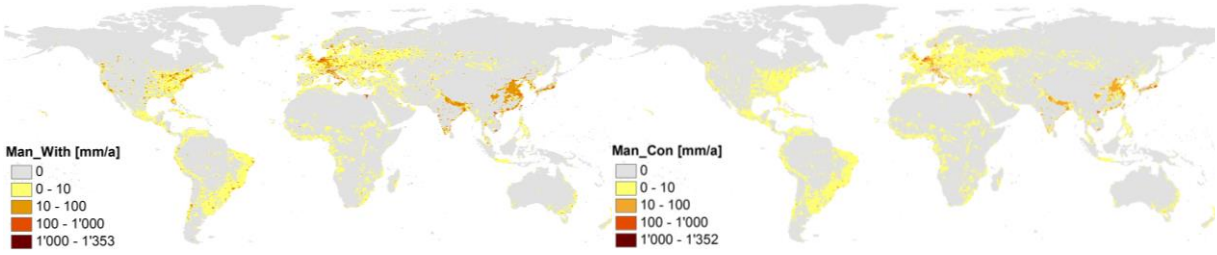

Figure 14: Water withdrawal (top) and consumption (bottom) for manufacturing purpose in mm/year for the year 2000. Spatial resolution of 0.5° x 0.5°. (CEH Information gateway).

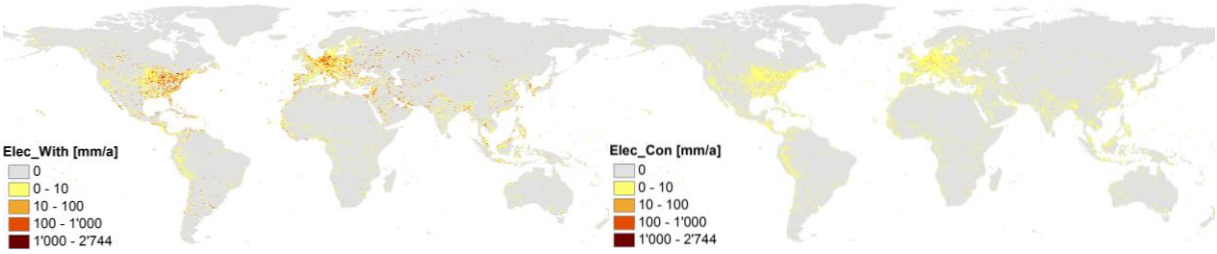

Figure 15: Water withdrawal (top) and consumption (bottom) for electricity production in mm/year for the year 2000. Spatial resolution of 0.5° x 0.5°. (CEH Information gateway).

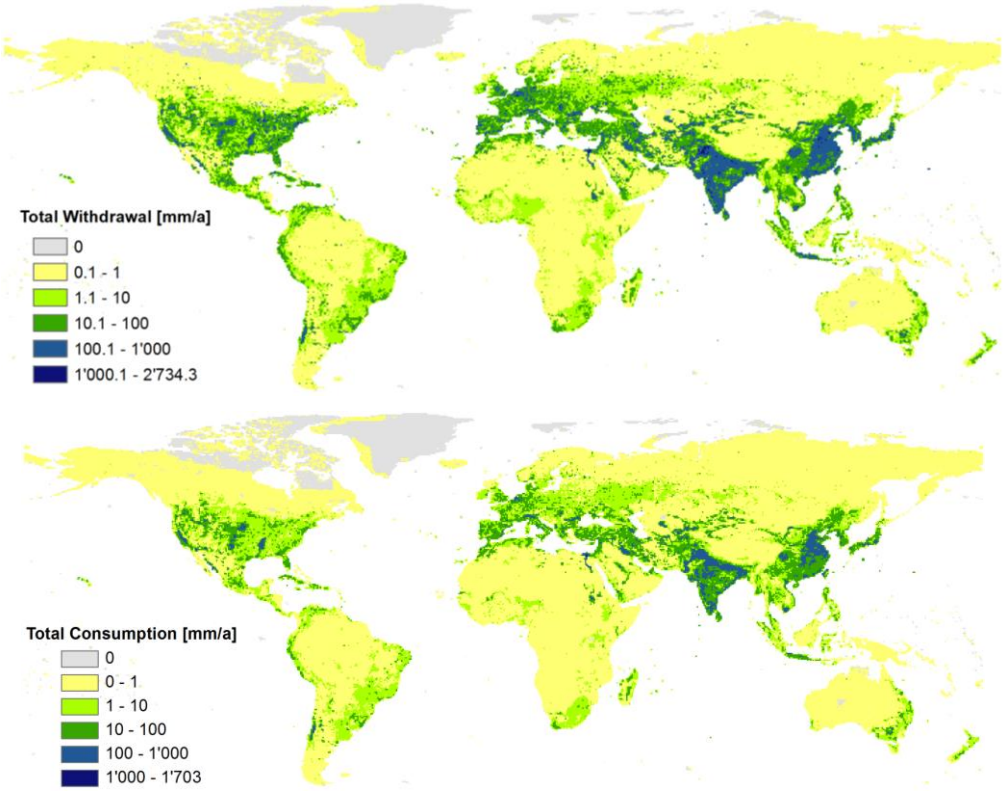

Figure 16: Total annual water withdrawal (top map) and consumption (bottom map) in mm/year for the year 2000 with a spatial resolution of 0.5° x 0.5°. The total withdrawal and consumption, respectively, is computed by summing all sectors.

3.2 Data processing

In order to make the withdrawal and consumption data (from WATCH) given in mm/month and mm/s comparable to the water availability data it has to be transformed into m^3/month or m^3/year and aggregated to watershed level. Therefore the water use of each grid cell has to be multiplied with the cell area [km^2/grid cell] and with 1000 times the number of seconds within a month or a year in order to obtain [m^3/grid cell/month] or [m^3/grid cell/year], respectively. For each watershed these cell values are summed up in order to obtain the sectoral and total water use on watershed level. The global water withdrawal and consumption is computed by summing up the withdrawals and consumptions, respectively, of all watersheds.

The total global water withdrawal for the year 2000 amounts to 3896 km3/year. Irrigation accounts for 71% of the total global withdrawal and for 85% of the total global consumption (see Table 6). With 14% of the total withdrawal, electricity production is the second largest sector on a global scale, but the smallest measured by consumption (1%). Global total consumptive use is 35% of total withdrawal. For regions with extensive irrigation this consumptive share is higher,

while in regions with electricity production as the dominant water use sector, the share is considerably lower (see Appendix Figure 49).

Table 6: Global sectoral and total annual water consumption and withdrawal for the year 2000 in km³/a.

	Withdrawal [km³/a]	Fraction of total withdrawal [%]	Total consumption [km³/a]	Fraction of total consumption [%]
Irrigation	2754	71	1150	85
Domestic	331	8	53	4
Manufacturing	257	7	107	8
Electricity	526	14	13	1
Livestock	27	1	27	2
Total	3896	100	1352	100

The annual global values agree with the values found in literature. According to Wada et al. (van Beek, Wada et al. 2011) the global water withdrawal amounts to 3700 km³/a , 68.6 % (2538 km³/a) account for agricultural water withdrawal. This is very close to the values found when the WATCH data is summed up (see Table 6). Rost et al. (2008) find a global blue water consumption of 1364 km3/a and a withdrawal of 2555 km/a for agriculture only, which again is in the same range as indicated by the data downloaded from WATCH.

The global monthly irrigation and total withdrawals are plotted in Figure 17. The modelled withdrawals are not constant over the year. Even on a global scale withdrawal exhibits a considerable sub-annual variation due to variable water use for irrigation (withdrawals for other sector are assumed to be time constant over a year.).

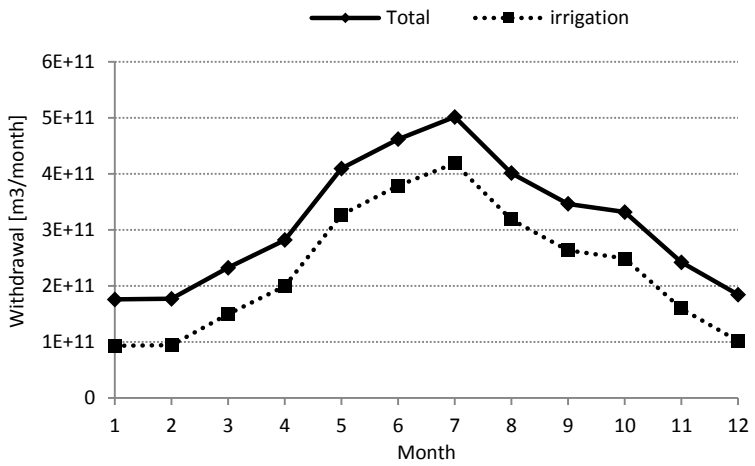

Figure 17: Global monthly irrigation and total withdrawal according to the WaterGAP WATCH for the year 2000.

Figure 18 to Figure 22 depict the global annual water use pattern for the different sectors on watershed level. The total annual water withdrawal is visualized in Figure 23. In arid and semi-arid regions, irrigation is the dominant water use sector, accounting for more than 90% of total withdrawal. In Europe (except southern Europe), Canada and eastern USA less than 10% of withdrawals are used for irrigation. In these regions the predominant water use sector is the electricity production, accounting for more than 50% of total withdrawal.

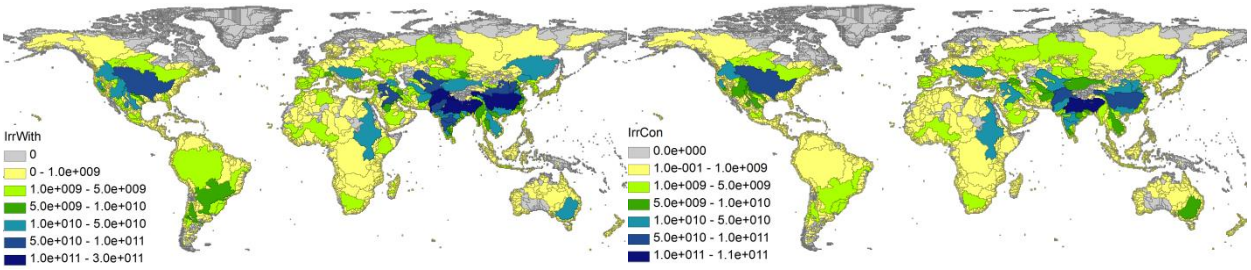

Figure 18: Annual water withdrawal (left) and consumption (right) for crop irrigation per watershed for the year 2000 in m³/year.

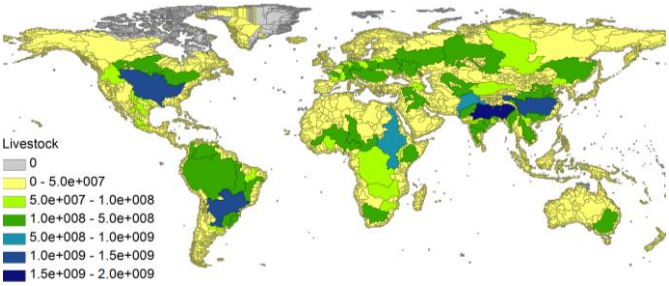

Figure 19: Annual water withdrawal and consumption respectively for livestock per watershed for the year 2000 in m³/year.

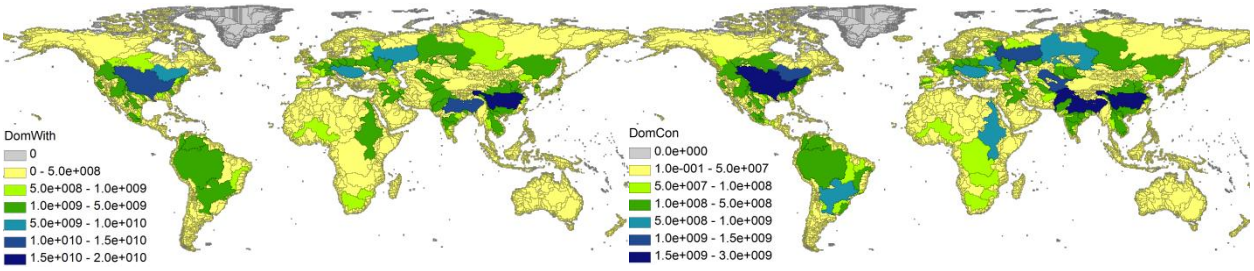

Figure 20: Annual domestic water withdrawal (left) and consumption (right) per watershed for the year 2000 in m³/year.

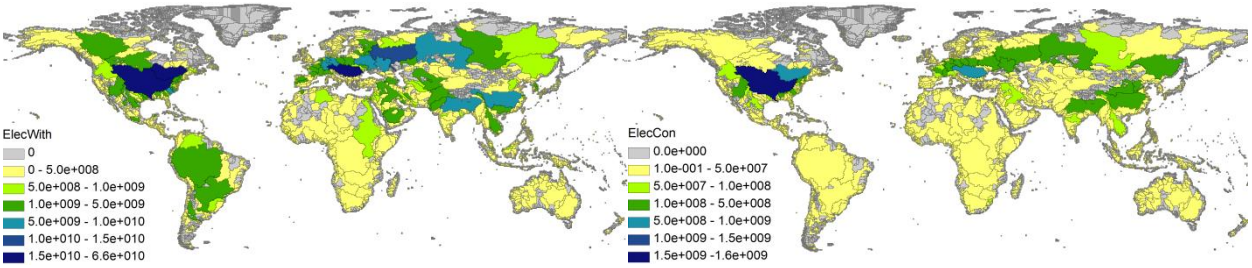

Figure 21: Annual water withdrawal (left) and consumption (right) for electricity production per watershed for the year 2000 in m³/year.

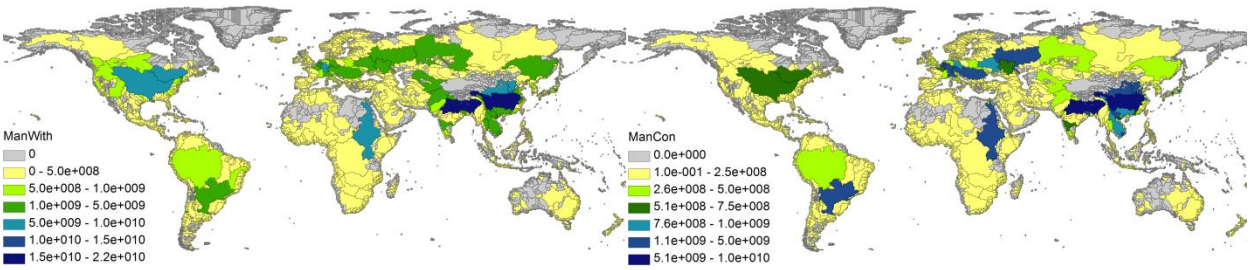

Figure 22: Annual water withdrawal (left) and consumption (right) for manufacturing purpose per watershed for the year 2000 in m³/year.

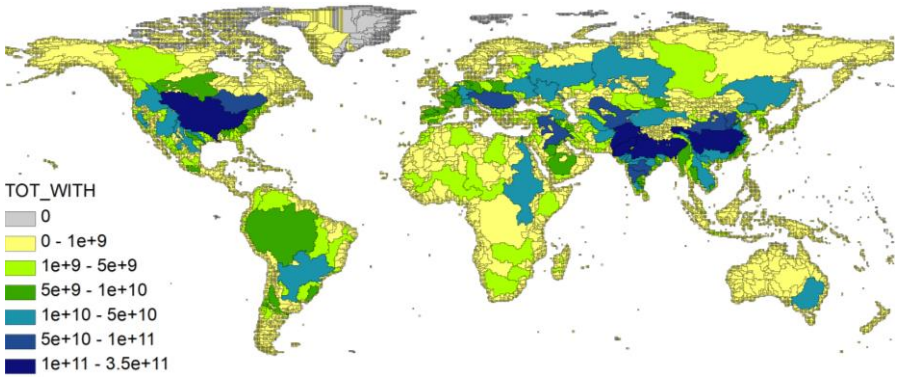

Figure 23: Total annual withdrawal per watershed for the year 2000 in m³/year.

Figure 24 plots the monthly withdrawal variation as an example for the Mississippi, the Nile and the Amazon watershed. It becomes evident that in watersheds, where the irrigation sector is dominant (Mississippi, Nile), withdrawal can vary considerably during the year.

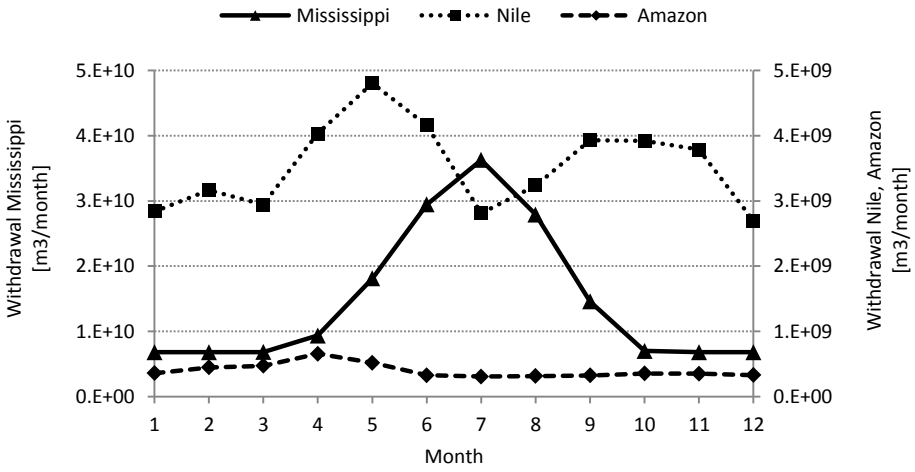

Figure 24: Monthly withdrawal according to the WaterGAP model in the Mississippi, the Nile and the Amazon watershed for the year 2000.

4 Data Validation

4.1 Comparison of Watch WaterGAP and Alcamo WaterGAP model output

As mentioned earlier certain hydrological and water use model input parameters haven been standardize in the context of the WATCH project. Consequently the WaterGAP output data by WATCH differ from the WaterGAP output provided by Alcamo.

Table 7 lists the differences in WaterGAP input data. The data has not been analysed in detail. The variables forcing the water use model are listed in Table 5.

Table 7: Differences in Water GAP input data comparing Alcamo et al. (2003) and WATCH (WATCH modelling protocol)

Input parameter	WaterGAP Alcamo	WaterGAP WATCH
Soil map	FAO 1995, Version 3.5	Harmonized world soil map (IIASA, FAO)
Drainage direction map	DDM30 ((Döll, P., and Lehner, B. (2002))	DDM30 (Döll, P., and Lehner, B. (2002)) mapped to the CRU land surface mask
Lakes, reservoir, wetland	Compilation of geographic information (Lehner and Döll, 2001)	Global land and wetland database (GLWD1) (Lehner , B. and Döll, P. (2004))
Land sea mask	IMAGE 2.2 land mask	0.5° CRU
Climate data	New et al. (monthly values 1901-1995)	WATCH Forcing Data (WFD) (Weedon 2010, 2011) (1963-2001)
Computed discharge	Actual discharge (considering human impact)	Naturalized discharge: reservoirs are not considered; human impact run considers water use, dam

Figure 25 shows the ratio of the annual mean water availability published by Alcamo to the annual mean water availability published by WATCH. Values below 1 indicate an overestimation of availability by the WATCH data compared to the data provided by Alcamo. It is obvious, that the WATCH data tend to overestimate the availability for the arid zones (especially Northern Africa, Saudi Arabia and Middle East) compared to the WaterGAP data by Alcamo. The discrepancies in the availability data can only partially be explained by the fact, that WATCH reports the natural discharge (without human interventions such as dams or withdrawal) and Alcamo the actual discharge (considering human impact) (see Appendix Figure 50).

Another reason might be that WATCH uses an uncalibrated and Alcamo a calibrated version of the WaterGAP model. The WaterGAP, model used by Alcamo et al. (2003), has been tuned for 724 drainage basins worldwide, based on observed discharges. The tuning basins cover about 50% of the global land area (excluding Greenland and Antarctica). The goal of the calibration process was to minimize the difference between the modelled and observed long-term average discharges. Only the vertical water balance for the land area has been tuned by adjusting the runoff coefficient of the total land-runoff equation. The coefficient was adjusted homogeneously for all cells within each watershed. In 385 basins a satisfactory agreement of modelled and observed discharge has been achieved by adjusting the runoff coefficient within the physically plausible range. In the other 339 basins, the discharge was either underestimated (mainly snow dominated areas) or overestimated (mainly semi-arid and arid regions). For those watersheds a runoff correction factor is assigned to each cell within the watershed. In some cases, the correction of the cell runoff still did not lead to an acceptable model result. A second correction factor has been applied directly to the discharge at the measurement station. In basins where such correction factors had to be introduced, the model does not correctly simulate the dynamics of the water cycle. It rather serves to interpolate the observed discharge in space and time. Figure 52 in Appendix 9 displays the basins for which the model can be calibrated by adjusting the runoff coefficient within physically plausible limits. A more detailed description is provided by Alcamo et al (2003) and Döll et al. (2002).

It is recommended to further analyse the climate data in order to identify the source for the discrepancies.

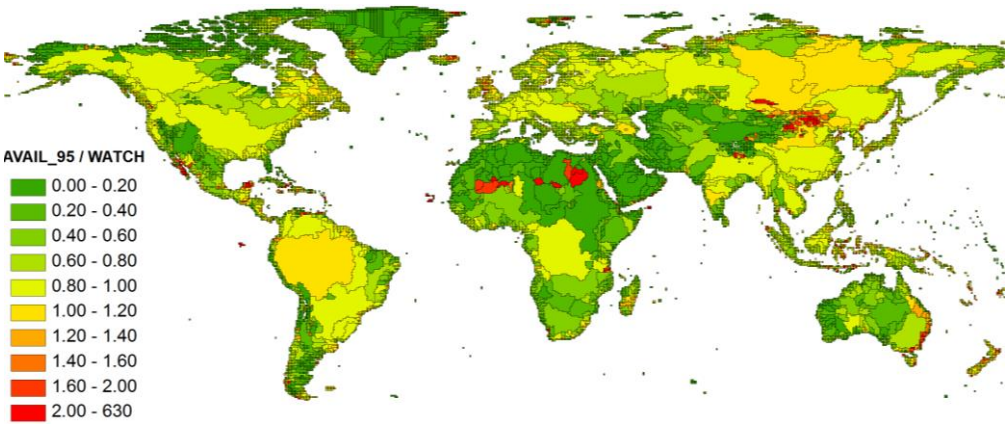

Figure 25: Comparison of WaterGAP output data published by Alcamo and WATCH. The map visualizes the ratio of Alcamo (Availability_95) to WATCH annual mean availability.

Figure 26 shows the ratio of the annual mean water withdrawal published by Alcamo to the annual mean water withdrawal published by WATCH. Values below 1 indicate an overestimation of withdrawal by the WATCH data compared to the data provided by Alcamo. It is obvious, that the WATCH data tend to underestimate water withdrawal compared to the data reported by Alcamo.

The discrepancies may arise on the one hand due to the different input data in the water use model and on the other hand due to different climate data. Climate is an important driver for irrigation water requirement as well as for water availability.

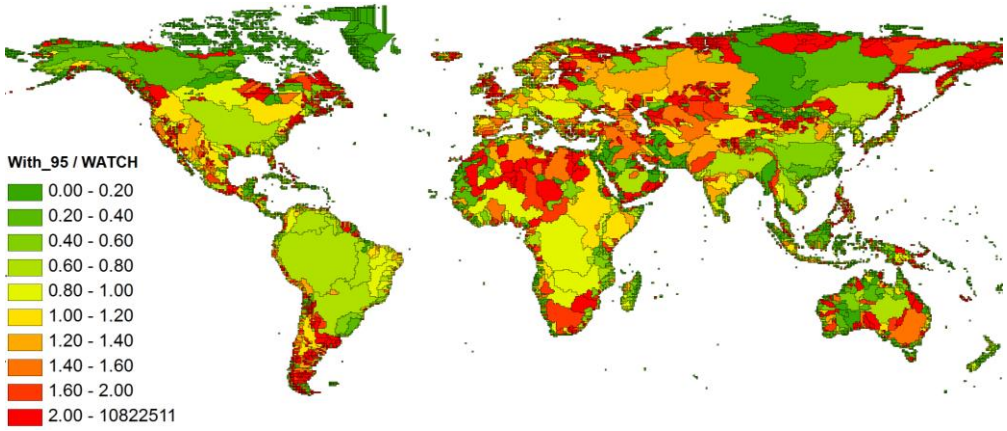

Figure 26: Comparison of WaterGAP withdrawal output data published by Alcamo and WATCH. The map visualizes the Alcamo (Withdrawal_95) to WATCH withdrawal ratio.

4.2 Validation with literature values

Validation of the WaterGAP availability and withdrawal data with observed and literature values reveal that water availability in arid and semi-arid areas tends to be overestimated by the global hydrological model (WGHM of WaterGAP). The modelled discharge for the Nile basin for example is ten times higher than the observed discharge. Even if the water consumption is taken into account, the simulated and observed value differs by more than a factor of five. According to Döll et al. (2002) the model formulation of WGHM is likely to be incomplete for these regions. For example, losses from the river to groundwater, or the evapotranspiration from many small ephemeral ponds forming after rainfall are not taken into account. These processes are likely to be relevant in the Nile, the Niger, the Senegal and the Orange basins for example.

The model seems to perform well for Western and Central Europe.

In order to verify the simulated water use it is recommended to aggregate the values at country level rather than at watershed level, as water use data are mostly reported at national scale.

Table 8 lists the WaterGAP output data (discharge and water use) by WATCH and Alcamo as well as observed values for a selection of watersheds.

Table 8: Comparison of modelled and observed discharge.

Watershed	Modelled (WaterGAP WATCH)						Modelled (WaterGAPAlcamo)		observed	
	Discharge†	Withdrawal					Discharge†††	Withdrawal	Discharge	Use
		Total††	Agri	Dom	Elec	Man		Total		
	[km3/a]	[km3/a]	[km3/a]	[km3/a]	[km3/a]	[km3/a]	[km3/a]	[km3/a]	[km3/a]	[km3/a]
Nile	447	44 (27)	34.3	3.6	0.6	5.3	76	53	39 (grdc 87 asawan)	68 (FAO Egypt only)
Niger	309	3.6 (1.6)	2.5	0.7	0.1	0.3	147	3	177 (Wikipedia)	
Congo	1412	0.8 (0.2)	0.2	0.5	0.0	0.07	1349	0.7	1247 (480 km to outlet)	
Senegal	33	1.6 (0.7)	1.4	0.1	0.1	0.0	5.7	0.6	21.7 (grdc 1903-1974 207 km to outlet)	
Orange River	24	3.5 (1.5)	2.2	0.7	0.2	0.3	8.4	6.3	4.6 (grdc 1964-1986 197 km to outlet)	
Indus	197	189 (69)	182	3.7	2.4	0.4	121	240	208 (Wikipedia)	299 (FAO)
Huanghe	50	71 (24)	60.5	4.5	0.2	5.6	56	52	45 (grdc at 679km to outlet) Qn: 56; Qm: 30 (Wang 2006)	28.5 (consumption)
Seine	20	7.1 (2)	1.1	1.5	3.5	1.1	17	9	17 (Wikipedia)	
Loire	34	5.2 (1.8)	2.1	0.8	1.9	0.4	32	5	26 (grdc 1863-1979)	
Rhône	56	7.2 (1.7)	1.9	1	3.8	0.6	54	6	53 (grdc 1920-1979)	
Garonne	39	6.8 (2)	2.8	0.5	3.4	0.2	31	4	20 (wikipedia)	
Rhine	81	19.5 (5)	0.9	3.5	9.4	5.6	80	23.5	71.8 (grdc 1930-1997)	
Guadalquivir	18	5.3 (2.7)	4.4	0.5	0.3	0.1	6	8.5	9.9 (grdc)	
Danube	234	61 (18)	28.5	6.5	21.8	4	215	57	204 (grdc 1921_1985)	
Volga	375	24.2 (0.5)	3.8	5.7	11.9	2.8	234	33	255 (grdc)	
Mississippi	641	182 (63)	96.4	13.8	66.1	5.9	531	127	555 (grdc)	
Rio Grande	25	14.4 (6)	10.7	1.6	1.7	0.5	8	15	3.6 (grdc 1900-1972 454 km to basin outlet)	
Colorado	31	15.1 (8)	12.2	1.2	1.2	0.5	1.5	19	0.7 (grdc 165-1975 274 km to outlet)	
Amazon	6230	5.2 (1.5)	1.7	1.3	1.5	0.8	6802	3.7	5865 (grdc)	

† Natural discharge, human impact is not considered
†† Withdrawal values, consumption values in brackets/parentheses
†††Actual discharge, considering human impact

5 Water Stress Index WSI

Water stress is defined by the ratio of total annual freshwater withdrawal to hydrological availability (WTA), or the ratio of total annual freshwater consumption to hydrological availability respectively (CTA) (Pfister, Koehler et al. 2009).

Moderate and severe water stress occurs above a WTA of 0.2 and 0.4, respectively. These figures are expert judgments and the threshold for sever water stress might vary from 0.2 to 0.6.

5.1 Annual WSI

5.1.1 Method

To calculate the Water Stress Index (WSI), the availability and use (withdrawal and consumption) data as described in section 0 and 3.2 are used to describe the WTA ratio of 11'558 individual watersheds with global coverage.

The Water Stress Index (WSI) is adjusted to a logistic function to achieve continuous values between 0.01 and 1:

$$WSI_{WTA} = \frac{1}{1 + 99 \cdot e^{-6.4 \cdot WTA \cdot VF}} \quad (2)$$

Where *WTA* is the watershed specific mean annual withdrawal to availability ratio and *VF* is the watershed specific variation factor, which is included in order to account for the temporal variability of water availability. Monthly and annual variability of precipitation may lead to increased water stress during specific periods, if insufficient water storage capacities are available (e.g. dams, lakes, reservoirs). Such increased stress cannot be compensated by periods of low water stress. *VF* corrects for this increased effective water stress, which differentiates watersheds with strongly regulated flows. VF is derived from the standard deviation of the monthly and annual precipitation data. The logistic function is tuned to result in a WSI of 0.5 for a WTA of 0.4, which is the threshold between moderate and severe water stress. A WTA of 0.2 and 0.6 result in a WSI of 0.09 and 0.9, respectively. For more details consult Pfister, Koehler et al. (2009).

The total global average consumption to withdrawal ratio of the used data is 37%. The consumption based Water Stress Index WSI_{CTA} is thus calculated according the equation (2 as described above replacing WTA by CTA/0.37:

$$WSI_{CTA} = \frac{1}{1 + 99 \cdot e^{-17.4 \cdot CTA \cdot VF}} \quad (3)$$

where CTA is the watershed specific consumption to availability ratio. A CTA of 0.15 results in a WSI of 0.5, which is the threshold between moderate and severe water stress.

5.1.2 Results and Discussion

Figure 27 and Figure 28 visualize the withdrawal based WSI and the consumption based WSI, respectively, using the Watch WaterGAP data.

The computed Water Stress Index indicates high pressure on water resources for the west coast of USA, Chile, Middle East, India, Pakistan and West and East China. The water stress for Northern Africa is unexpectedly low, especially for the Nile basin. This is mainly due to the overestimation of the discharge by the global hydrological model.

For Saudi Arabia the withdrawal induced water stress is larger than the consumption based. These areas reveal a relatively low consumptive share (amount of consumed water relative to the amount of withdrawn water) (see Appendix, Figure 49). The dominant water users are the manufacturing sector as well as the electricity production. These are both sector with a relatively low consumption to withdrawal ratio.

For southern Europe as well as for western USA (Colorado basin) and the Tigris, Murray-Darling and Aral Sea basin on the other hand the consumption based WSI is bigger than the withdrawal based WSI. These areas are dominated by a high consumptive share due to intensive irrigation. The agricultural sector accounts for more than 80% of the total consumed water.

For quality issues withdrawal based WSI might still be the better choice. Withdrawal can be interpreted as an indication for structure density (e.g. hydropower, dams or reservoirs) which have a significant influence on monthly availability, as well as an increased potential for evaporation losses. Additionally released water has generally a lower quality (physical and chemical impairments). The consumption based WSI on the other hand is more relevant for statement on quantitative water scarcity.

It is important to mention, that the WSI does not make a statement about the actual water availability or risk to water-stress. Watersheds with a low WSI do not implicitly have a lot of water available. It rather indicates that the actual water use is minor compared to availability. Already a small increase in withdrawal might lead to water stress.

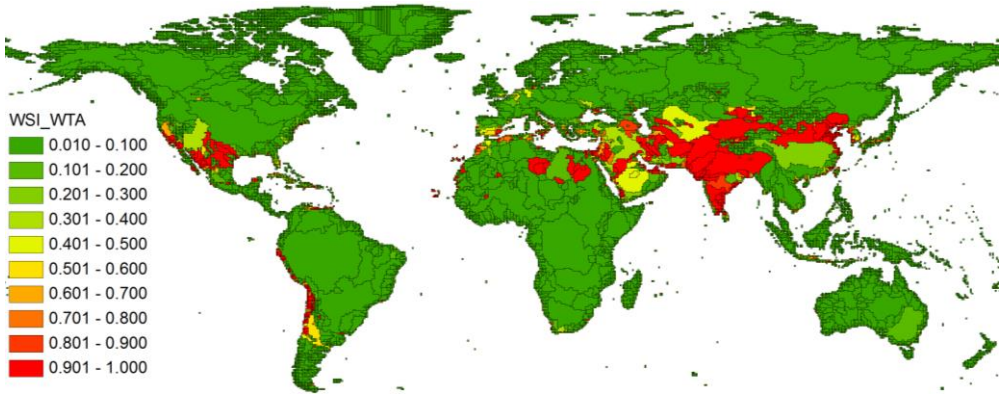

Figure 27: Withdrawal based Water Stress Index (WSI_{WTA}) [m^3/m^3] calculated based on WATCH data from WaterGAP data

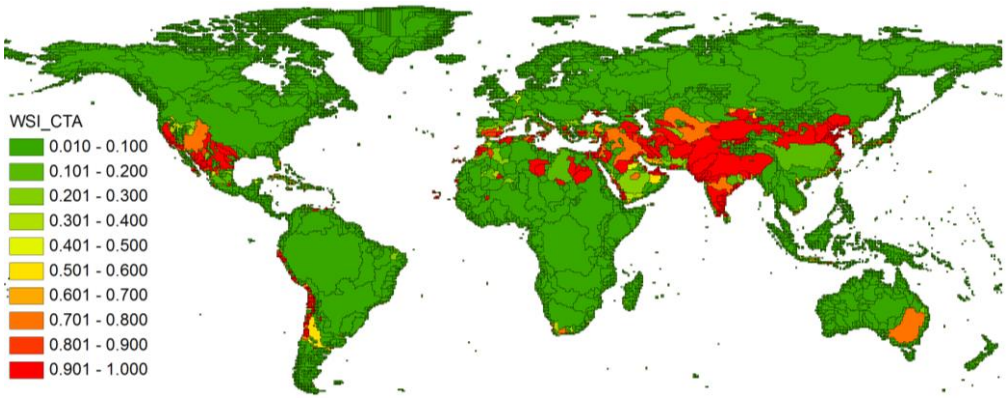

Figure 28: Consumption based Water Stress Index (WSI_{CTA}) [m^3/m^3] calculated based on WATCH data from WaterGAP data

Figure 29 depicts the withdrawal based WSI calculated based on the WaterGAP data provided by Alcamo et al (2003). The water stress is higher compared to the one estimated with the Watch data, especially in Northern Africa and other arid areas.

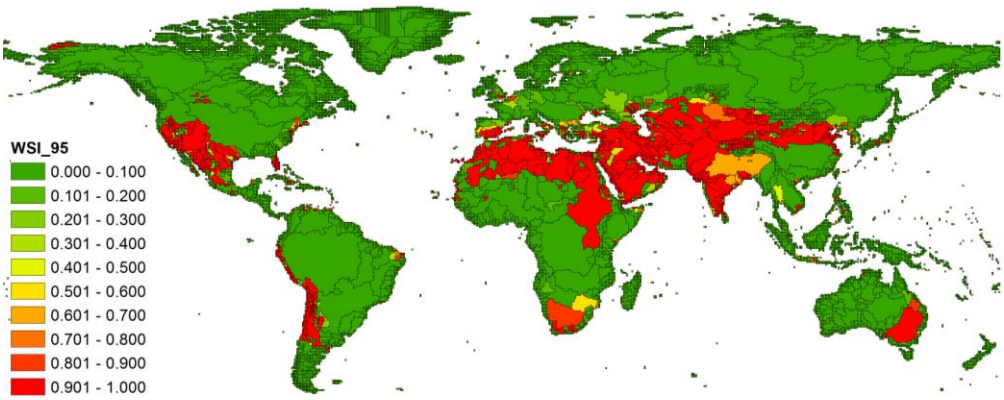

Figure 29: Withdrawal based Water Stress Index [m³/m³] calculated based on WaterGAP model data provided by Alcamo aggregated to the watershed level used by WATCH.

5.2 Monthly WSI

The annual WSI based on the approach of Pfister, Koehler et al. (2009) as described in section 5.1.1 includes a term for temporal variability of water availability (VF) in order to account for increased pressure in watersheds with unstable water supply over time. The monthly component of this factor has been excluded as it is explicitly covered by applying monthly WSI. Only the inter-annual variability is accounted for by the geometric standard deviation of annual precipitation data during the "climate normal period" (1961-1990) within watershed basin. The global mean variation factor accounting for inter-annual variability only (VF_m) is 1.5 times smaller than the one included in the annual WSI function. Consequently the monthly WSI function of each watershed *J* is adjusted by replacing VF by $VF_{m,J}$·1.5:

$$WSI_{i,J} = \frac{1}{1 + 99 \cdot e^{-9.8 \cdot WTA_{i,J} \cdot VF_{m,J}}} \qquad (4)$$

Where $WTA_{i,J}$ is the watershed specific mean annual withdrawal to availability ratio and VF is the watershed specific variation factor

5.2.1 Results and discussion

Figure 30 visualizes the monthly withdrawal based Water Stress Index. The monthly WSI indicates that the water stress can vary considerably over a year. Furthermore it shows that many watersheds are at least partially affected by water scarcity. In the Mississippi basin for example, the simulated pressure on the water resources is high during the month of June, July and August while for the rest of the year the pressure is low. This is mainly caused by the high water withdrawal (see Figure 24) and the declining discharge (see Figure 10) during these months. But also Spain and the Murray-Darling basin in Australia are partially affected by high water stress.

However, storage processes in lakes, groundwater, snow/ice and reservoirs is not accounted for on watershed level and needs to be done in future research. For regions with high groundwater storages the seasonal variation of availability (and consequently WSI) is expected to be overestimated by the current model.

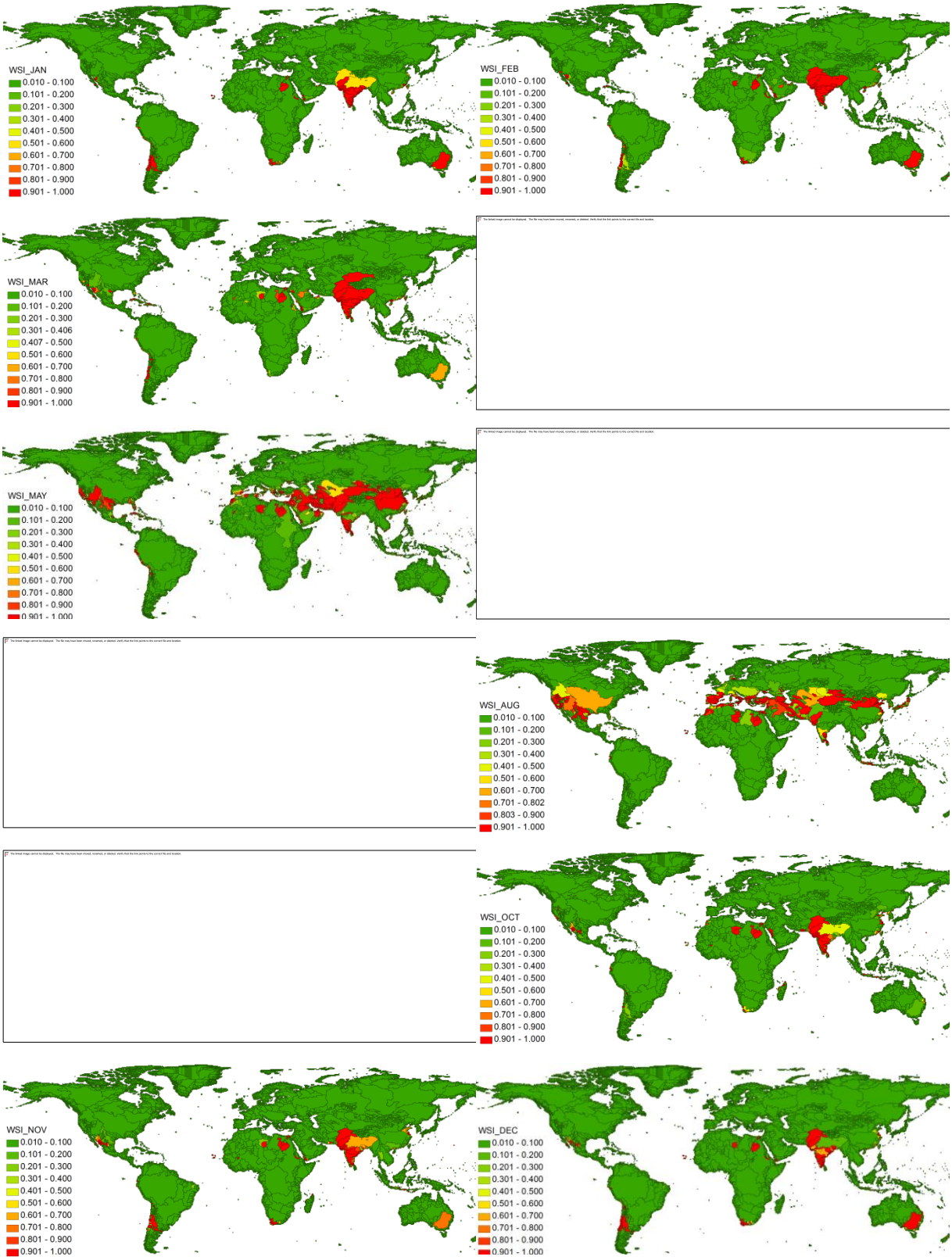

Figure 30: Monthly withdrawal based WSI [m³/m³] (January to December from top left to bottom right), calculated based on the WATCH data

6 Groundwater

6.1 Groundwater availability

6.1.1 Literature

The importance of quantifying groundwater recharge to allow for a sustainable groundwater use has been acknowledged in literature (Döll and Fiedler 2008: 870). Döll and Fiedler (2008 p. 864) state that even though groundwater recharges surface water bodies in most regions of the world it is useful to quantify groundwater availability separately *"first, they* [groundwater resources] *are much better protected from pollution than surface water resources. Second, the use of groundwater resources is much less restricted by seasonal or inter-annual flow variation than the use of surface water"*. They emphasize that *"as expected, because of its longer residence times, groundwater can decrease the seasonal variations of total water storage"* (Döll and Fiedler 2008: 870). Hence, *"groundwater recharge is equivalent to renewable groundwater resources"* Döll and Fielder (Döll and Fiedler 2008: 863). In particular, they outline that *"in semi-arid and arid regions, mountainous regions, permafrost regions and in the Asian Monsoon region, groundwater recharge accounts for a lower fraction of total runoff, which makes these regions particularly vulnerable to seasonal and inter-annual precipitation variability and water pollution."*

Groundwater recharge data on a country level has been collected in different databases (e.g. by the World Resource Institute or the FAO). However, Döll et al. (2008) argue that these groundwater recharge estimates are to be used with precaution because *"country values of groundwater recharge have been obtained by very diverse methods"* (Döll and Fiedler 2008: 864) and in different decades ranging back to the 70s. Acknowledging the difficulties in measuring groundwater recharge, a modelling approach seems reasonable. In the following a short overview of recent literature in the field of groundwater recharge modelling and model estimates is given. There are two main publications quantify groundwater recharge based on hydrological models. The first by Döll and Fiedler (2008) is based on the WaterGAP Global Hydrology Model WGHM (Alcamo, Döll et al. 2003). The second one by Wada et al. (2010) uses the hydrological model called PCR-GLOBWB (van Beek and Bierkens 2008).

<u>Groundwater recharge modelled with WaterGAP (WGHM version 2.1)</u>

The groundwater recharge in WaterGAP is modelled by partitioning the total cell runoff into a fast surface and a subsurface runoff as well as groundwater recharge. This is done following a heuristic approach based on qualitative knowledge about the influence of certain characteristics on the partitioning of total runoff: relief, soil texture, hydrogeology (hydraulic conductivity) and the occurrence of permafrost and glaciers (Döll et al. 2000 and Döll and Fiedler 2008: 866). These coefficients are determined based on expert guesses followed by iterative adjustment. Groundwater recharge is generally modelled as diffuse groundwater recharge. *"Only diffuse groundwater recharge is taken into account […] as groundwater recharge from surface water bodies cannot be estimated at the macro-scale"* (Döll and Fiedler 2008: 863). Döll and Fiedler (2008) use two different precipitation datasets (CRU and GPCC) and outline that precipitation is the major driver for groundwater recharge. They recommend using the mean between the results obtained with the two precipitation datasets as neither of them is preferable to the other one.

The estimation of groundwater recharge was found to be more difficult for arid than for humid regions *"mainly due to the small values of these variables"* (Döll and Fiedler 2008: 867). For the former, the groundwater recharge model was therefore adapted Döll et al. (2008). For semi-arid and arid regions groundwater recharge was for instance assumed to only occur above a certain precipitation threshold [10mm/d]. Döll and Fiedler (2008: 865) acknowledge that *"other hydrological models as well as the land surface schemes of climate models also compute variables that could be considered as diffuse groundwater recharge"* but add that the groundwater recharge component is mostly *"lumped with interflow"* and *"model outputs have not yet been analysed ant interpreted at the global scale".*

The model results of Döll and Fiedler are used in the "World-wide Hydrogeological Mapping and Assessment Program" WHYMAP (Döll and Fiedler 2008: 876). It was found to be difficult to validate the model in a satisfying manner due to lack of validation measurement data. *"Due to scarcity of reliable independent information on groundwater recharge at all scales* […] *it is difficult to judge how well the computed groundwater recharge estimates correspond to realty"* (Döll and Fiedler 2008: 876). Nevertheless, it seems reasonable to use the output data of this model as the currently best available data as for the other models for which data is provided within the WATCH project the diffuse groundwater recharge has not been analysed, interpreted and published at all.

For the PCR-GLOBWB model on the other hand Wada et al. (2010) did analyse and publish groundwater recharge results but the model is not included in the WATCH project and hence, data is not available. Nevertheless, the groundwater recharge as modelled with PCR-GLOBWB is shortly outlined below.

Groundwater recharge modelled with **PCR-GLOBWB**

The most recent estimate on groundwater recharge has been published by (Wada, van Beek et al. 2010). The *"map of groundwater recharge shows very similar patterns"* (Wada, van Beek et al. 2010: 2). In the study of Wada et al. (2010) the groundwater recharge is given as a yearly mean and amounts to $15.2*10^3$ km³/year. This is 20% more than found by Döll and Fiedler (2008) who estimate the total global groundwater recharge to be $12.7*10^3$ km³/year even though the total runoff is smaller in the latter case. Wada et al. (2010) explain that the main difference between their study and the work of Döll and Fiedler (2008) concerns the *"partitioning between surface runoff/interflow and baseflow"* Wada et al. (2010: 2). The latter is larger in the study of Wada et al. (2010). The aim of his study is to quantify groundwater depletion. Therefore, groundwater recharge and groundwater abstraction are quantified. The analysis is limited to *"sub-humid to arid areas"* (Wada, van Beek et al. 2010: 1). However, the groundwater recharge is simulated globally and given in the supplementary material. Wada et al. (2010) use the CRU precipitation dataset. The model approach is similar to the one of Döll and Fiedler (2008). "The total specific runoff of a cell consists of saturation excess surface runoff, melt water that does not infiltrate runoff from the second soil reservoir (interflow) and groundwater runoff (baseflow) from the lowest reservoir. Recharge from streams is not included in this model and hence it also is diffuse groundwater recharge.

In the following the WaterGAP WGHM is used because it is available in the WATCH project.

6.1.2 Data processing

In the following different data sources and the treatment of the data is explained. As a starting point Petra Döll was asked to provide their published results (Döll and Fiedler 2008) in digital form. She sent us a shape file containing information on the groundwater recharge [mm/year] using the CPU and the GPCC precipitation dataset as forcing data. Furthermore the shape file contains for each 0.5° x 0.5° grid the area over which they assume the water to infiltrate. In ArcMap this data is converted into a raster using the conversion function of the ArcToolbox. The visualization of the data as provided by Petra Döll is shown in Figure 31.

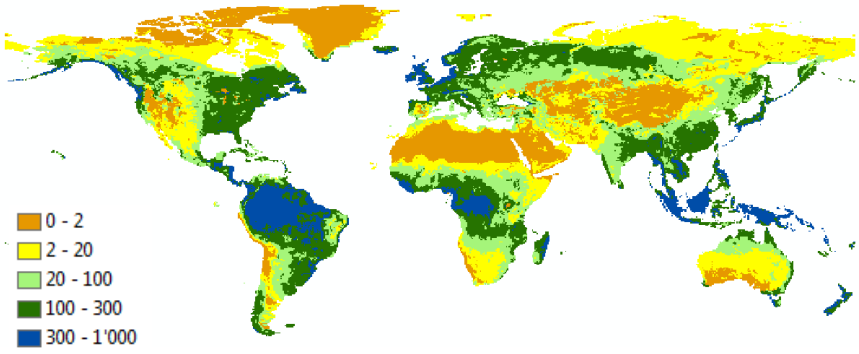

Figure 31: Groundwater recharge [mm/a] according to Döll and Fiedler (2008).

The values shown in Figure 31 are then converted into [m3/year] by multiplying them by 1000 times the area [km²] indicated in the file provided by Petra Döll. The results obtained are shown in Figure 32 for the average results using the CPU and the GCPP datasets as well as for the results obtained when only using the CPU precipitation dataset. It has to be noted that the legend now has a different scale not being comparable to the figure above. Yoshide Wada was also contacted and provided the groundwater recharge data he published as an ascii file (see Figure 33).

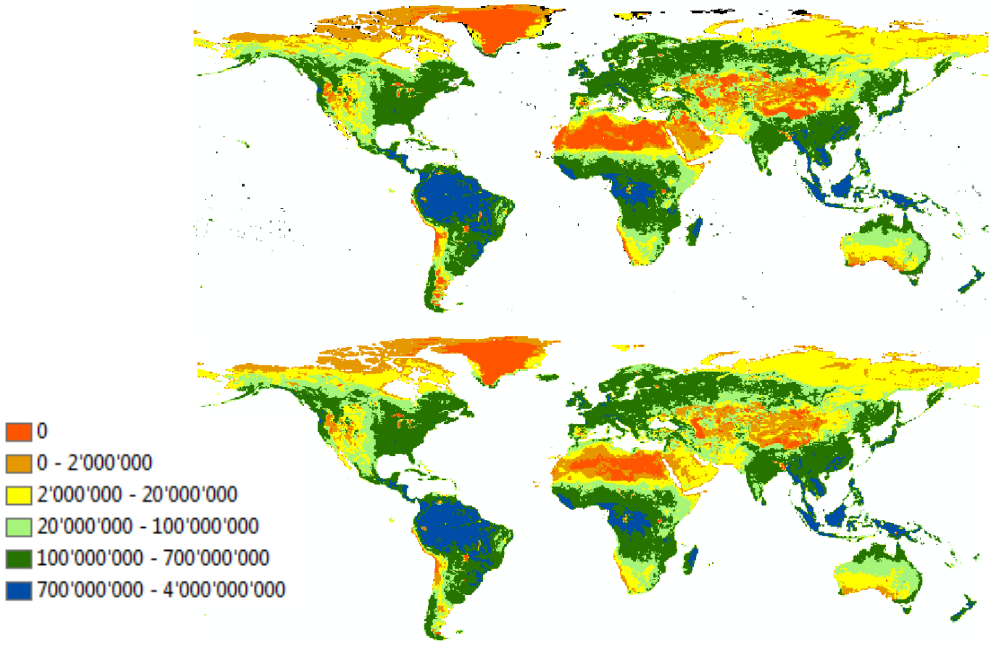

Figure 32: Data provided by Petra Döll converted from [mm/a] into [m³/a] once for the average results using the CPU and the GCPP precipitation data (top) and once only using the CPU precipitation data (bottom).

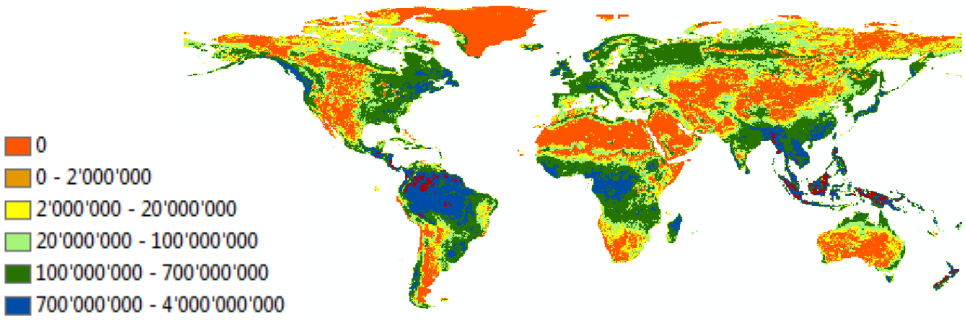

Figure 33: Groundwater recharge [m³/year] according to the data sent to us by Yoshihide Wada. Wada et al. (2010: 2) conclude that their *"results show very similar patterns as the one by Döll and Fiedler (2008).*

Instead of using the groundwater recharge data sent to us by Petra Döll it would be preferable to use the data provided in the WATCH project for the WaterGAP model. First, this seems to be the most consistent approach because the same forcing data (precipitation and temperature) as well as the same time period is used as for the discharge data. Second, the data is provided in daily time steps instead of a yearly average. And third, other models could if desired, also be considered.

WATCH subsurface flow runoff (Qsb)

WATCH reports model outputs separately for the surface (Qs) and the subsurface runoff (Qsb). The surface runoff includes *"runoff from the land surface and/or subsurface storm flow. This variable should include the fast component of runoff response. This includes any surface runoff generated as infiltration excess runoff or saturation excess runoff (or the parameterized equivalent). In addition it should include any subsurface lateral quick-flow, which based on modelers experience is best routed as a fast storm-flow component, rather than a drainage or base-flow component"* (EU WATCH Sixth Framework Programme 2007-2011) The subsurface flow on the other hand *"should include the slow drainage component of runoff response. This includes gravity drainage and slow response lateral flow. Ground water recharge will have the opposite sign"* (EU WATCH Sixth Framework Programme 2007-2011). The unit of both variables is mm/s. The data download and the visualization of netCDF data in ArcMap is explained in the previous chapters. As for the discharge data, as a matter of consistency only non-leap years are analysed.

The raw netCDF data that was downloaded and stored. The Matlab codes reading this data and aggregating it to daily averages across different years and on watershed level. The content of this code is summarized in Figure 34. The output data is given in km^3/year. It is read by the Matlab code "Summary_Results/GW_to_Discharge" which converts the results to m^3 per average day of the corresponding month and stores them in Excel files.

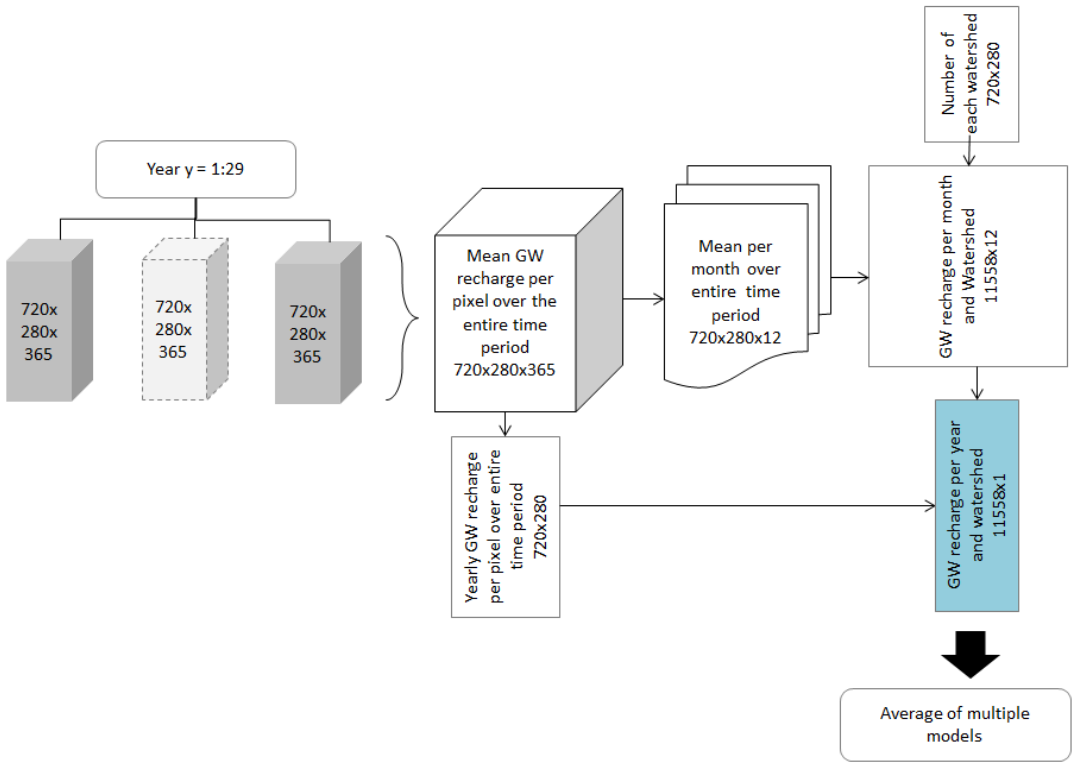

Figure 34: Explanation of the Matlab code summing up the groundwater recharge over each of the 11558 watersheds

The global yearly groundwater recharge is given in Table 9 and the monthly recharge is plotted in Figure 35.

Table 9: Global annual mean groundwater recharge (Qsb) for different models for the time period 1963 to 2001 calculated based on the Watch data.

Model name	Global groundwater recharge [E+13 m3/a]
WaterGAP	1.28
JULES	1.75
H08	4.18
LPJmL	2.79

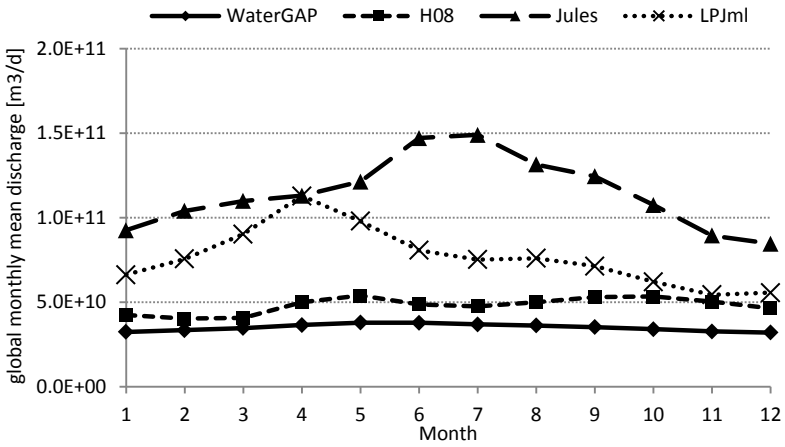

Figure 35: Global monthly mean groundwater recharge (Qsb) for the time period 1963 to 2001 for different models given in m3/average day within the corresponding month.

Figure 36 is a visualisation of the yearly subsurface runoff obtained from the WATCH data for the WaterGAP model. In some regions the recharge is smaller than the recharge published by Döll (see Figure 32) (e.g. Amazon, Congo) and in other region it is larger (Northern Africa, Spain, Saudi Arabia, Mongolia, Kazakhstan, Middle East and Australia). These Discrepancies correspond with the differences found when comparing the total discharge data from Watch with the one from Alcamo and might arise due to the fact, that different forcing data (precipitation and temperature) have been used. Nevertheless, the overall pattern is very similar.

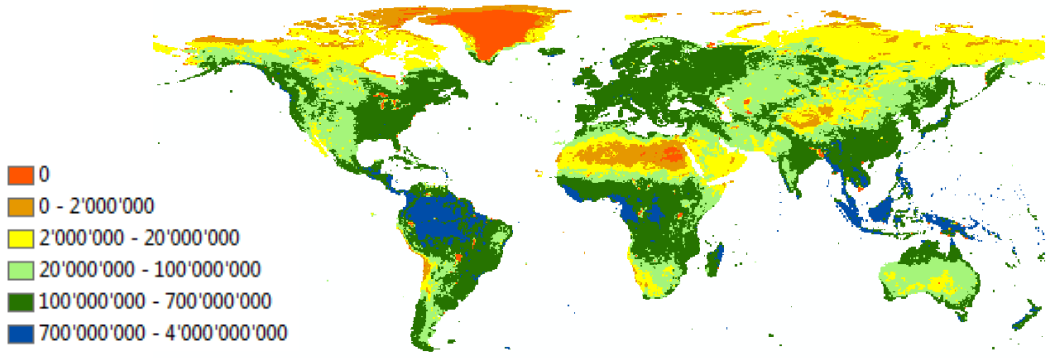

Figure 36: Annual mean groundwater recharge per pixel [m³/a] for the time period 1963 to 2001 calculated based on the Watch WaterGAP recharge data (Qsb).

Figure 37 contains the same information for the H08, the Jules and the LPJml model. When it comes to slow subsurface runoff (Qsb) or groundwater recharge the WaterGAP model is assumed to perform better than the other models. Within the WATCH project it is the only one for which groundwater recharge data was specifically analysed. Döll and Fiedler (2008) write that *"Other hydrological models as well as the land surface schemes of climate models also compute variables that could be considered as diffuse groundwater recharge. To our knowledge, however, these model outputs have not yet been analysed an interpreted at the global scale."* Dieter Gerten (co-developer of the LPJml model) agreed that *"WaterGAP uses a more elaborate approach in that they consider more explicitly the groundwater recharge (related to geological features)"* (Personal Email from 5.March 2012).

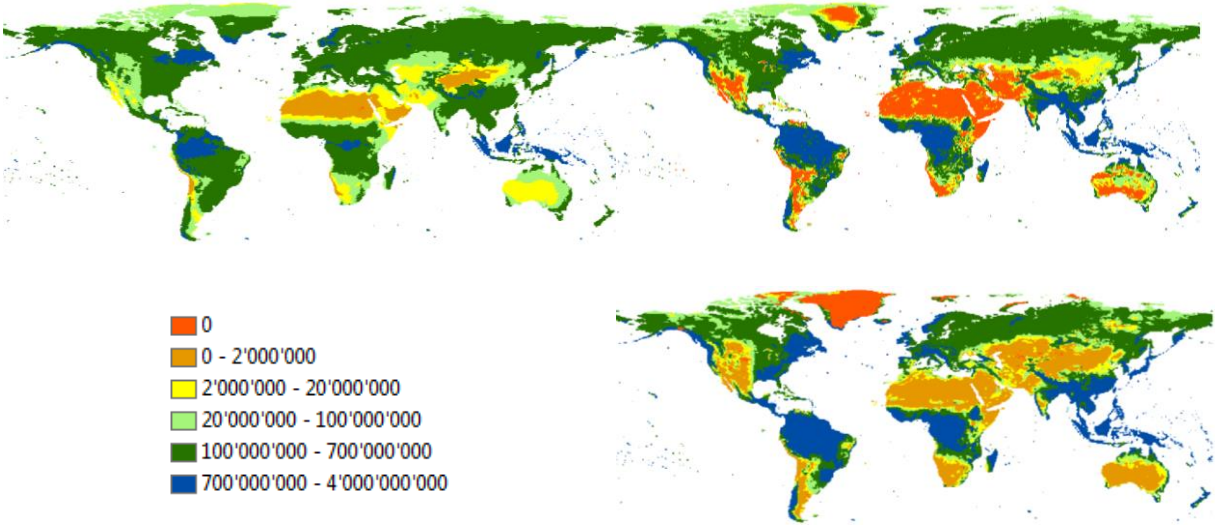

Figure 37: Slow subsurface runoff (Qsb) downloaded from Watch for the H08, the LPJml and the Jules model given in [m3/year]

According to the WaterGAP WATCH model results (see Figure 35) there are no large sub-annual variations of the global groundwater recharge. However, on a watershed level there are substantial sub-annual variations. These variations are expressed by computing the percentage of the difference between the average monthly and the average yearly discharge to the total yearly discharge:

$$\frac{\sum_{i=1}^{m}(nr_{days_i} * |dailyGW_i - dailyGW_{year}|)}{365 * dailyGW_{year}} \cdot 100 \qquad (5)$$

Where m is the number of months, nr_days_i is the number of days in the respective month, $dailyGW_i$ is the groundwater recharge on an average day in the respective month and daily GWyear is the groundwater recharge on an average day considering the entire year.

Figure 38 indicates for each watershed the percentage obtained with Equation (5. As opposed to Figure 35 it becomes clear that the groundwater recharge (even though it appears about time invariant on a global scale) shows significant sub-annual variations on a watershed level.

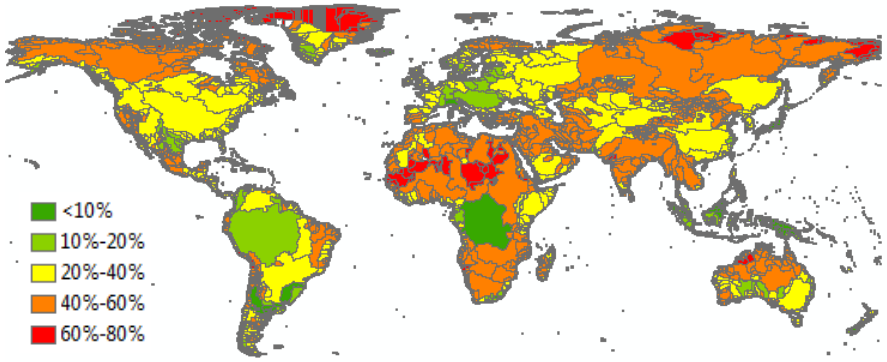

Figure 38: The ratio of the difference between the average monthly and the average yearly recharge to the total yearly recharge obtained with equation (5.

Figure 39 plots the monthly groundwater as well as the total discharge variations as an example for the Mississippi (25%), the Nile (40%) and the Amazon (16%) watershed. It becomes evident that the variation in the groundwater recharge is smaller than in the total discharge.

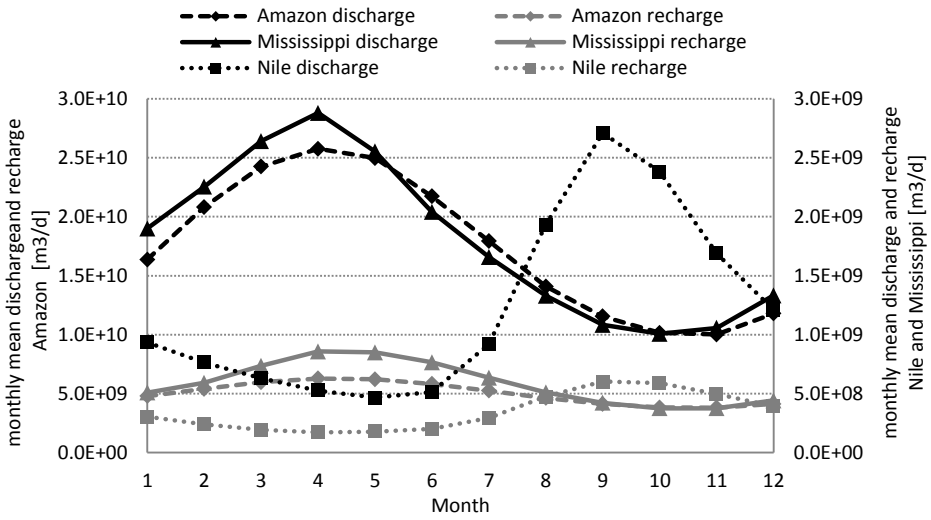

Figure 39: Monthly mean discharge (black) and groundwater recharge (grey) for the time period 1963 to 2001 according to the WaterGAP WATCH model in the Mississippi, the Nile and the Amazon watershed.

Figure 40 shows the simulated groundwater recharge as a fraction of the simulated discharge by the Watch WaterGAP model. The computed recharge fraction is highest for Eastern Europe and Murray-Darling watershed in Australia.

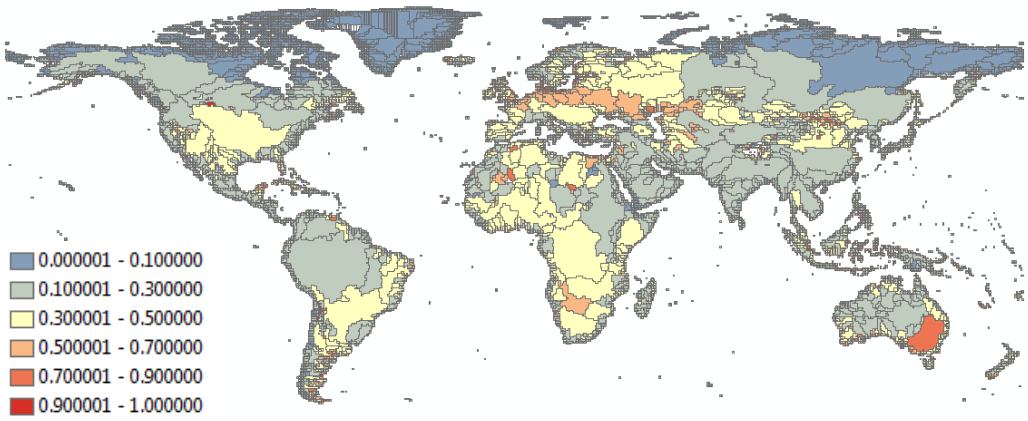

Figure 40: Groundwater recharge fraction. GW recharge according to the Watch WaterGAP (Qsb) data (long term from 1963-2001 without leap years) to the total discharge according to Watch WaterGAP data.

6.2 Groundwater withdrawal and consumption

6.2.1 Literature

In recent years a number of authors published articles in the field of estimating the water sources accessed. A short overview of these publications is given below.

Hanasaki et al. (2010) estimated the ratio of blue water to total water during the cropping period (only agricultural water use is looked at). They further differentiate between tree sources of blue water withdrawal used for agriculture. The first one is stream flow as well as large reservoirs (>10^9m^3) that are *"individually geo-referenced"* (Hanasaki, Inuzuka et al. 2010: p.233). The second one is medium-size reservoirs (with a storage capacity between 10^6 m^3 and 10^9m^3). These two sources (= Precipitation – Evapotranspiration) sum up to the renewable blue water resource. Renewable groundwater is *"implicitly treated and included in stream flow because soil is modelled with a depth of 1m and soil water movement from the upper 1m soil to the lower is automatically included in subsurface flow"* (personal communication). The third source comprises non-renewable and nonlocal blue water (NNBW) including groundwater, seawater desalination and water that is deviated from other sources. Naota Hanasaki provided us with an ascii file containing these water use fractions. Unfortunately the three water source categories as given by Hanasaki et al. (2010) cannot be used for our purposes because they do not differentiate between surface water and groundwater used.

An interesting approach to estimate groundwater withdrawal in agriculture is followed by **Siebert et al. (2010)**. Other water use sectors such as water use in the domestic or manufacturing sector are not considered. Siebert et al. (2010) *"present a new global inventory on the extend of areas irrigated with groundwater, surface water or non-conventional sources, and determine the related consumptive water uses"* Siebert et al. (2010). They use national and subnational *"census based statistics from international and national organizations"* (Siebert, Burke et al. 2010). It has been found that 38 % of the irrigated area is equipped for groundwater irrigation consuming 43 % of the consumptive water use for irrigation. Siebert et al. (2010: p. 1873) outline that *"in theory many surface water irrigation systems should be able to provide water at lower cost than groundwater, where pumping cost may be substantial"*. However, they conclude that surface water irrigation is uncertain and unpredictable and that *"availability of groundwater may be taken as an indicator of probable or potential use of groundwater in irrigation*" (Siebert, Burke et al. 2010: p. 1873). Furthermore, it is stated that *"the preference for groundwater or surface water us also related to tenancy, with private schemes more often irrigated with groundwater and public or state farms more often irrigated with surface water"* (Siebert, Burke et al. 2010: p. 1874). Another influence factor outlined by Siebert et al. (2010) is the crop type, *"with vegetables often irrigated with groundwater and staple cereal crops cultivated at the large scale more often irrigated with surface water"* (Siebert, Burke et al. 2010: p. 1874). They proposed a framework predicting the water source used based on the availability of groundwater taking into account the aquifer conditions as well as climatic conditions. In order to test the framework Siebert et al. (2010: p. 1875) compare the areas that are equipped for groundwater irrigation with the *"continental groundwater resource maps of the World-wide Hydrogeological Mapping and Assessment Programme (WHWMAP, available at www.whymap.org)"* containing information on the aquifer typology and the (major groundwater basin, complex hydrological structure and local and shallow aquifer) as well as on groundwater recharge classes. It is shown that groundwater is more readily used where major groundwater basins are present. Regarding groundwater recharge, it could

be shown that groundwater is most frequently used in regions with a medium groundwater recharge. In regions with a high recharge it can be assumed that *"enough rainfall is available for crop production*" (Siebert, Burke et al. 2010: p. 1875). The proposed simplified framework is found to lead to suitable results.

We asked Stephan Siebert why he describes his framework only for irrigation and whether it could not be applied to water use in general (including domestic and surface water use). He answered that in general it is true that *"this simplified framework should work for other sectors as well. However, in reality it is not that simple because other factors impact the type of water use as well. For large scale irrigation development you need usually huge volumes of water while for other sectors quality parameter and a stable supply are more important. Therefore, irrigation was traditionally more based on surface water resources while the small volumes of domestic or manufacturing water use were more often withdrawn from groundwater bodies. This is changing because we find today more and more supplementary irrigation in more humid regions as well. Here the volumes of water needed are much smaller than the volumes consumed in the traditional more arid irrigation regions. The technological development makes it also much easier to use groundwater today as compared to the situation 50 years ago. Therefore there is also a historical dimension in the development. Another factor is the question of who can control the use of water resources. Groundwater use is usually more under the control of farmers or local industries or local water suppliers while the use of surface water from reservoirs can much easier be controlled by a central government"* (Personal communication).

Furthermore, we asked whether they already calculated and/or published the results for the water sources used according to the framework they propose (globally and with a high spatial resolution, e.g. per country, river basin or higher). He said that they *"did not try to simulate ground- and surface water use based on the proposed framework. It is certainly not so easy to define the required thresholds and we would need to consider too many specific exceptions in different regions (e.g. sometimes groundwater use is restricted by laws etc.)"* (Personal communication). He refers to supplement S2 of their paper saying that *"we provide a table with volumes of groundwater and surface water used for irrigation at the national and subnational level (15038 administrative units). To compute this water use we used statistics on areas equipped for irrigation with groundwater or surface water and combined these data with a global crop water model."* It is in general worthwhile looking at the supplementary information to this publication. Supplement S1 for example lists available statistics in the field of water and groundwater use. And Supplement S2 could be used in order to estimate the water source used per country or on a subnational level.

Stefan Siebert provided us with a shapefile indicating the statistical units he uses. We are not allowed to pass this document on to other people because he does not possess the copyright for all the data contained in the shapefile.

Partly based on the publication of Siebert et al. (2010)**, Döll et al. (2011 (article in press))** recently published an estimate of different water sources used. In this publication the water withdrawal is separated into groundwater and surface water withdrawal. The water source fraction is assumed to be time invariant but dependent on the water use sector (irrigation, household and manufacturing). For livestock and cooling of thermal power plants it is assumed that the entire water use is covered by surface water.

The estimation of the water source is done differently for the three water use sectors. The groundwater use was estimated and the surface water use calculated by subtracting the groundwater use from the total water use. The fraction of groundwater use in agricultural irrigation is estimated by looking at the area that is equipped for groundwater irrigation. The information is largely derived from Siebert et al. (2010) but some small modifications were done by Döll et al. *"Groundwater fraction of domestic and manufacturing water use were estimated [...] mainly based on information from the International Groundwater Resource Assessment Center"* (IGRAC, www.igrac.net). However, in personal communication Prof. Dr. Döll expressed her concern regarding the scale and the large uncertainty of the results and said that if possible it was *"preferable to concentrate on irrigation"* because that data quality is better for irrigation than it is for domestic use and manufacturing. Petra Döll provided us with a shapefile containing the water use fractions for irrigation. As she finds data quality to be too poor she did not share the water use fractions for domestic and industrial water use with us.

Another estimate of water sources used was published by **Wada et al. (2010)**. The aim of this publication is to find the abstraction that is exceeding the recharge hence to indicate *"overexploitation or persistent groundwater depletion"* (Wada, van Beek et al. 2010: 1). They restrict their analysis to sub-humid to arid areas but results are provided for many regions in the world (compare to Figure 41). Wada et al. (2010) use the data in the IGRAC database to estimate the groundwater abstraction and no difference is made between different water use sectors because in IGRAC no such difference is made. Döll et al. (2011 (article in press)) outline that the amount of groundwater abstraction they find *"is twice the amount that was estimated by Wada et al. (2010)"* and add that *"Wada et al. (2010) used more limited information than we did to determine groundwater withdrawals. They relied exclusively on estimates of total, i.e. not-sector-specific groundwater withdrawals by country as collected by IGRAC."* Döll et al. (2011 (article in press): 11) The difference can partly be explained by the counties that are neglected by Wada et al. (2010) due to lack of data. But Döll et al. (2011 (article in press): 11) acknowledge that this does not explain the entire difference.

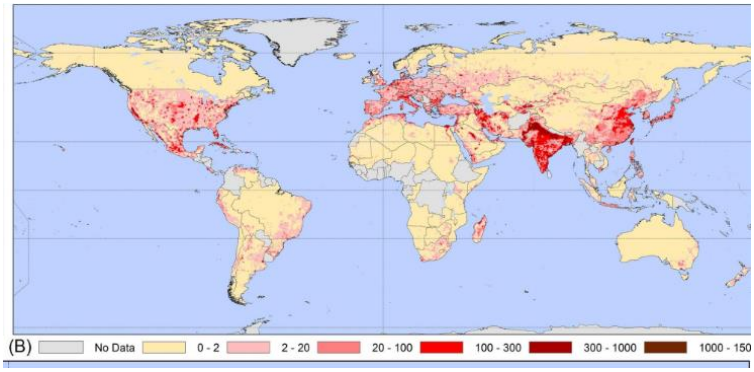

Figure 41: Groundwater consumption according to Wada et al. (2010).

In the following the treatment of the data published by Döll et al. (2011 (article in press)) is further explained. We would recommend using this data as it is more recent and extends the data available from the IGRAC (www.igrac.net) with additional international reports and national sources. So far Petra Döll only provided the data for the agricultural sector. However, it might be worthwhile to collaborate with her more closely.

6.2.2 Data processing

Siebert et al. (2010) use a shapefile with 15038 subnational units. He provided us with this shapefile as well as the groundwater use fraction and the absolute groundwater use for each of these subnational units. However, for the purpose of this study this data is not usable as the subnational units do not correspond with the definition of the 11558 watersheds. It seems reasonable to use the data published by Döll et al. (2011 (article in press)) directly as this data is a further development of the result of Siebert et al. (2010) when it comes to agricultural groundwater use.

Therefore we use the more recent data by Döll et al. This is largely based on the Siebert data but slightly improved in some regions. Also, the data is provided as a 0.5° x 0.5 ° shape file. The groundwater withdrawal fraction data is only available for pixels in which irrigation occurs. For the domestic and the manufacturing sectors we digitized the map of the groundwater withdrawal fraction for the domestic sector published by **Döll et al. (2011 (article in press)).**

First we converted the shapefile with the irrigation groundwater withdrawal fraction into a raster file using the Tollbox in ArcMap. We chose "maximum area" as a cell alignment type. However it should not be of any importance because all polygons are already 0.5° x 0.5° squares. Cell size is chosen to be 0.5° (see top left map in Figure 42). For the domestic groundwater withdrawal fraction we geo-referenced the TIFF file, extracted from **Döll et al. (2011 (article in press)),** and converted it into a raster file with a resolution of 0.5° x 0.5°. We used the colours for distinguishing six classes of groundwater withdrawal fraction. Since in the original map one colour does not represent a unique value but a range of groundwater withdrawal fractions we used the mean value of the range to assign to the corresponding colour. The top right map in Figure 42 visualizes the digitized map of the groundwater withdrawal fraction of domestic purpose. The total groundwater withdrawal fraction is computed as the ratio of the sum of the absolute groundwater withdrawal for irrigation, domestic and manufacturing sector (calculation see below) to the total water withdrawal of all sectors.

Groundwater fraction of water withdrawals for irrigation exceeds more than 80% in Central USA (Mississippi), Saudi Arabia, Northern Africa, Western India and Pakistan. In the Nile Basin, South Africa, Iraq (Tigris), south-east Asia, Venezuela and Colombia and North-west USA groundwater abstraction for irrigation accounts for less than 10% of total water withdrawal for irrigation.

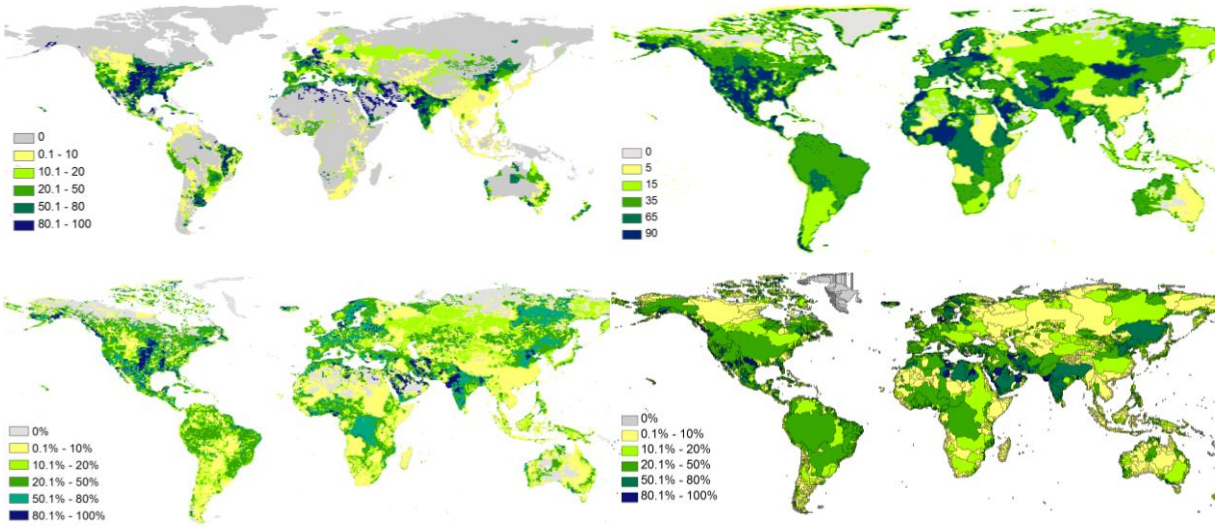

Figure 42: Groundwater withdrawal for irrigation in percentage of total surface and groundwater withdrawals for irrigation (top-left), groundwater withdrawals for domestic purposes in percent of total surface and groundwater withdrawals for domestic purposes (top-right), total groundwater withdrawals in percent of total withdrawals (bottom-left) and total groundwater withdrawals in percent of total withdrawals aggregated to watershed level (bottom-left). The total groundwater withdrawal fraction is computed as the ratio of the sum of the absolute groundwater withdrawal for irrigation, domestic and manufacturing sector (calculation see below) to the total water withdrawal of all sectors.

In order to obtain the absolute groundwater withdrawals for irrigation we multiplied the groundwater fraction of withdrawal with the total withdrawal for irrigation. The same procedure is applied for the domestic sector. The groundwater withdrawal for the manufacturing sector was estimated by multiplying the total withdrawal for manufacturing with the groundwater fraction of domestic withdrawal. Figure 43 depicts the absolute groundwater withdrawal values for the three water use sectors per pixel in [mm/a]. The sum of the three sectors is considered as the total groundwater withdrawal and is shown in Figure 44. The total surface water withdrawal is estimated as the difference between the total withdrawal and the total groundwater withdrawal.

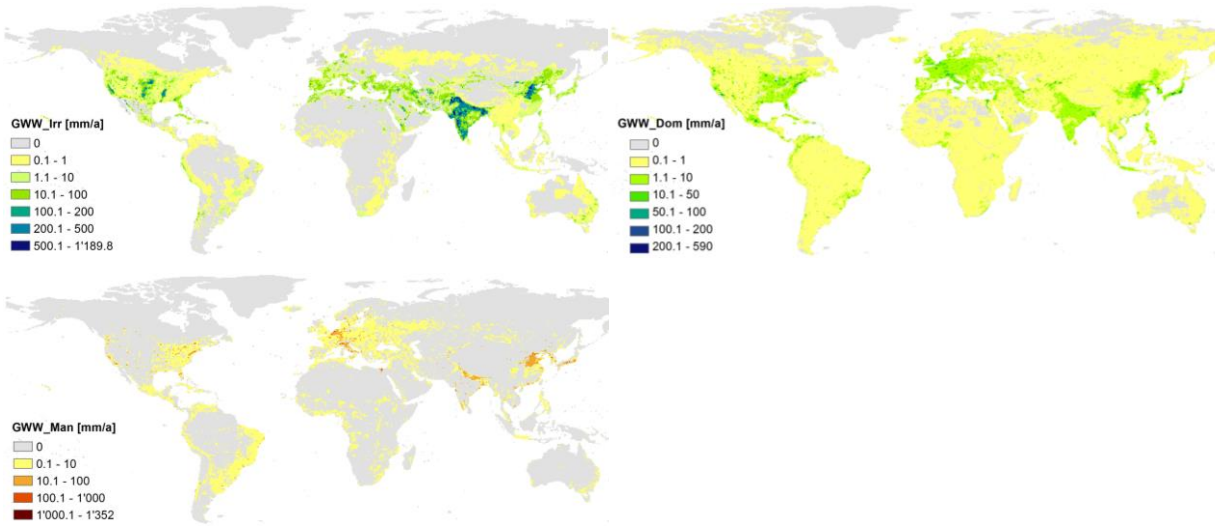

Figure 43: Absolute groundwater withdrawal for agricultural irrigation (top left), the domestic sector (top right) and for manufacturing purposes (bottom left) for the year 2000.

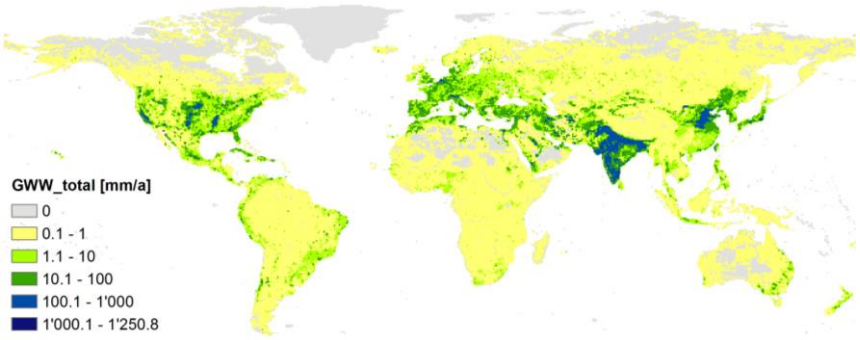

Figure 44: Total groundwater withdrawal (sum of irrigation, domestic and manufacturing withdrawal) for the year 2000.

We define the total groundwater consumption as the net groundwater abstraction, i.e. difference between groundwater withdrawals and return flows to groundwater. Return flows are assumed to occur only in irrigated areas due to the total irrigation water (taken from surface and groundwater). **Döll et al. (2011 (article in press))** defined a spatially resolute fraction of the return flows from irrigation which recharges groundwater. The total groundwater consumption per cell GW_{Con} is computed as:

$$GW_{Con} = (GWW_{irr} + GWW_{Dom} + GWW_{Man}) - f \cdot (Irr_{With} - Irr_{con}) \quad (6)$$

where GWW_{irr} is the groundwater withdrawal for irrigation, GWW_{Dom} is the groundwater withdrawal for domestic use, GWW_{Man} is the groundwater withdrawal for manufacturing use, f is the fraction of return flow from irrigation to groundwater, Irr_{With} is the total withdrawal for irrigation and Irr_{Con} is the total water consumption for irrigation.

The fraction of return flow f is a function of the fraction of irrigated area that is artificially drained. Return flow to groundwater is expected to be low in areas with artificial drainage systems. For more details consult **Döll et al. (2011 (article in press)).**

Surface water consumption is estimated as the difference between the total consumption and groundwater consumption. Groundwater consumption GW_{Con} and surface water consumption SW_{Con} can be positive or negative (see Figure 45). Negative values indicate a gain in stored water and positive values indicate storage losses. Groundwater stores can only increase in regions, where water for agricultural irrigation is mainly withdrawn from surface water bodies. Surface water stores can only increase in regions, with a high groundwater withdrawal fraction for the irrigation, domestic or manufacturing sector (reduced groundwater discharge to surface water due to decreased groundwater storage is not considered). South-east China, eastern India, Pakistan (Indus), Nile basin, South Africa and Chile are examples for regions with negative groundwater consumption (increased groundwater storage) and positive surface water consumption (decreased surface water storage). Central USA (Mississippi), north-western India and Central Europe are regions with positive groundwater consumption (decreased groundwater storage) and negative surface water consumption (increased surface water storage).

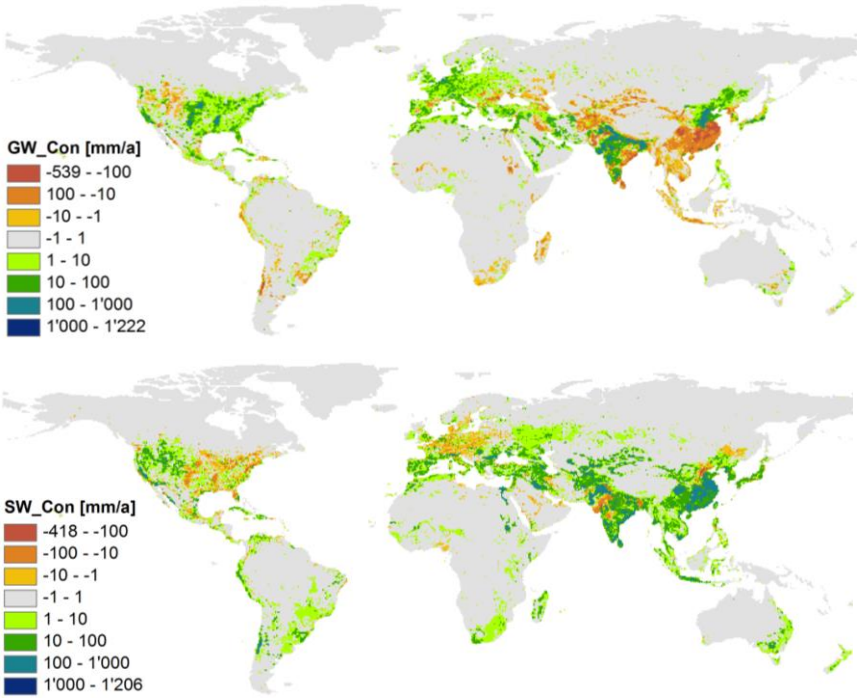

Figure 45: (top map) Total groundwater consumption in mm/a for the year 2000 obtained with equation (6 and (bottom map) total surface water consumption in mm/a for the year 2000, estimated as the difference between the total water consumption and the groundwater consumption. Negative consumption values imply storage increase.

Table 10 summarises the simulated global groundwater withdrawal for each sector as well as the total groundwater withdrawal and consumption. Globally the groundwater abstraction accounts for approximately 33% of total withdrawal but only for 18% of total consumption.

Table 10: Global sectoral and total groundwater consumption and withdrawal for the year 2000 in km³/a.

	Total withdrawal [km³/a]	Total consumption [km³/a]	Groundwater withdrawal [km³/a]	Groundwater consumption [km³/a]	Groundwater fraction of total with [%]	Groundwater fraction of total con [%]
Irrigation	2754	1150	1069	n.a.	42	n.a
Domestic	331	53	131	n.a.	40	n.a
Manufacturing	257	107	97	n.a	38	n.a
Electricity	526	13	0	0	0	0
Livestock	27	27	0	0	0	0
Total	3896	1352	1297	249	33.3	18

6.3 Water Stress Index for groundwater and surface water resources

6.3.1 Method

The specific withdrawal based Water Stress Index for the groundwater resource $WSI_{GW,WTA}$ is based on the following equation:

$$WSI_{GW,WTA} = \frac{1}{1 + 99 \cdot e^{-3.84 \cdot WTA\_GW \cdot VF}} \quad (7)$$

Where *WTA_GW* is the watershed specific mean annual groundwater withdrawal to groundwater recharge ratio calculated based on the data described in section 6.1.2 and 6.2.2. *VF* is the watershed specific variation factor and accounts for the temporal variability of water availability as described in section 5.1.1. The logistic function is tuned to result in a WSI of 0.9 for a WTA of 1, which is the threshold between sever and extreme water stress. It is assumed, that extreme water stress occurs when withdrawal exceeds recharge.

The total global average groundwater consumption to withdrawal ratio of the used data is 19%. The consumption based Water Stress Index for groundwater WSI_{CTA} is thus calculated according the equation (7 replacing WTA_GW by CTA_GW/0.19:

$$WSI_{GW,CTA} = \frac{1}{1 + 99 \cdot e^{-19 \cdot CTA\_GW \cdot VF}} \quad (8)$$

Where *CTA_GW* is the watershed specific mean annual groundwater consumption to groundwater recharge ratio calculated based on the data described in section 6.1.2 and 6.2.2.

The withdrawal and consumption based Water Stress Index for the surface water is calculated according the equation (2 and (3, respectively, by replacing WTA with WTA_SW and CTA with CTA_SW. The surface water withdrawal and consumption are calculated as described in section 6.2.2 . The surface water availability is assumed to be equal to the total availability total availability.

6.3.2 Results and Discussion

Figure 46 shows the computed withdrawal and consumption based Water Stress Index for groundwater, $WSI_{WTA,GW}$ and $WSI_{CTA,GW}$, respectively. WSI values above 0.9 imply groundwater depletion (withdrawal is larger than recharge). The pattern of the WSI for groundwater is similar to the one for the total water resources (see Figure 27). Only in Saudi Arabia the WSI for groundwater is considerably higher than the total WSI. For the Colorado, Tigris and Aral Sea Basin is slightly lower.

The Mississippi as well as Southern Europe and some parts of Northern Africa have a considerably higher $WSI_{CTA,GW}$ compared to $WSI_{WTA,GW}$ and the WSI_{CTA} for the total water recourses.

Figure 47 visualizes the withdrawal and consumption based Water Stress Index for surface water, $WSI_{WTA,SW}$ and $WSI_{CTA,SW}$, respectively. North and East-India, Saudi Arabia and the Middle East have considerably lower $WSI_{WTA,SW}$ compared to the total WSI_{WTA} and the $WSI_{WTA,GW}$. The same is true for the $WSI_{CTA,SW}$. Only in the Yangtze basin and in southeast-Argentina the it is higher.

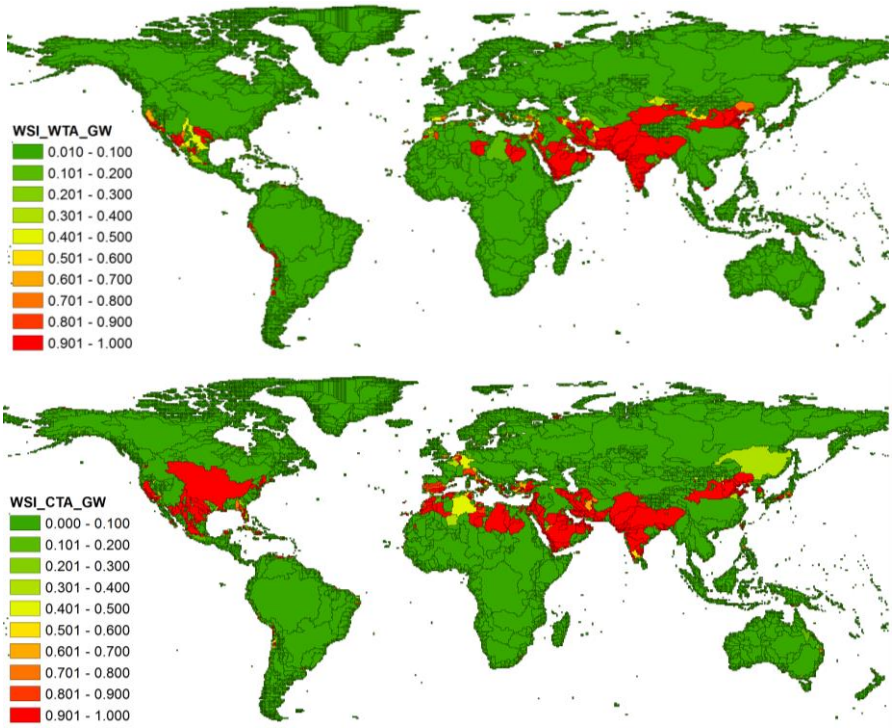

Figure 46: Withdrawal based Water Stress Index for groundwater ($WSI_{WTA,GW}$) (top map) and consumption based Water Stress Index for groundwater ($WSI_{CTA,GW}$) calculated based on the groundwater recharge data from WATCH and groundwater withdrawal fractions from Döll et al. (2011 (article in press))

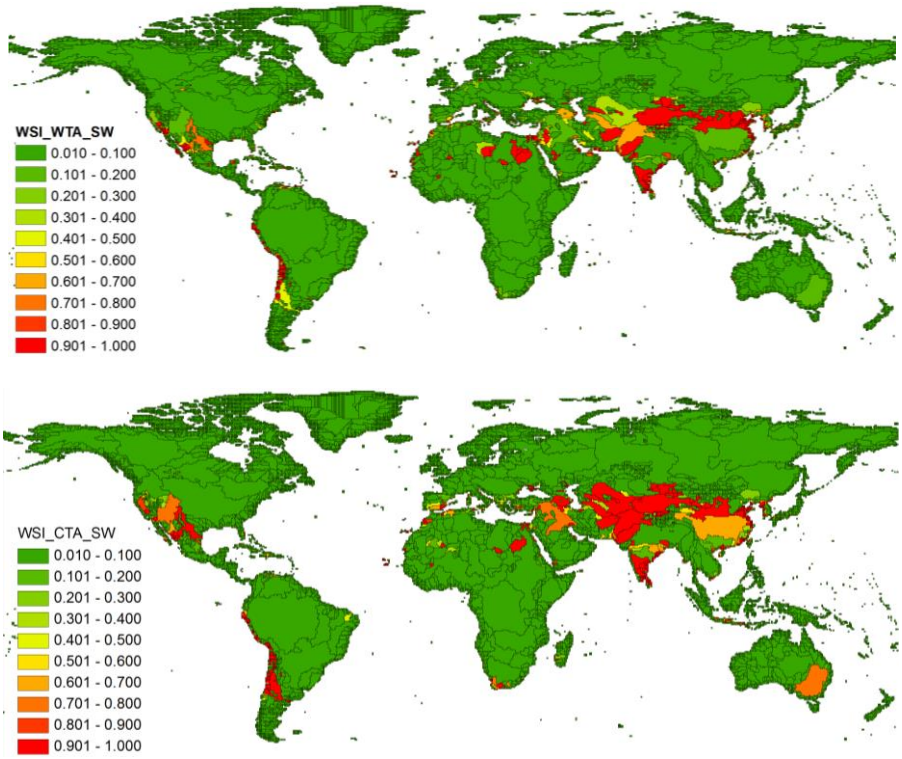

Figure 47: Withdrawal based Water Stress Index for surface water ($WSI_{WTA,SW}$) (top map) and consumption based Water Stress Index for surface water ($WSI_{CTA,SW}$).

7 Conclusion and Outlook

The study reveals that there exist considerable discrepancies between the basin discharges computed by the updated (WATCH) and the old (Alcamo et al. 2003) WaterGAP model as well as between the observed and the modelled discharge. Especially in semi-arid and arid regions the model performance is poor, as illustrated very strongly by the case of the Nile. The reasons are diverse. The model formulation of the global hydrological model is likely to be incomplete, especially for regions, where losses from the river to the groundwater, evapotranspiration from groundwater, evaporation from lakes (natural and artificial) and wetland or artificial water transfer are important processes in the water cycle. But also erroneous in input data, precipitation, in particular, as well as radiation, is a source for unsatisfying model performance.

Differences in the updated (WATCH) and old (Alcamo) WSI might arise due to:

- The fact, that WATCH uses an uncalibrated and Alacmo et al. (2003) a calibrated WaterGAP version (see section 4.1)
- Different definition of total availability: WATCH considers the natural availability and Alcamo the availability after human consumption (see section 4.1)
- Different land sea mask and drainage map
- Different forcing data, both climatic and water use variables

However, the results indicate the different problems of the sources of water abstraction as well as the fate of the release (withdrawal vs. consumption).

Another crucial result is the monthly WSI that are the first results on this temporal resolution with global coverage.

For the reasons state above we do not recommend the use of the updated WSI. This first phase of the project mainly revealed new questions that need to be addressed in future research.

7.1 Outlook for phase 2

7.1.1 General issue learned in phase 1

- More detailed and systematic validation of simulated discharge is required, as WaterGAP and other WATCH model performance seems to be poor especially for arid and semi-arid regions.
    - Contact and cooperate with model developers to gain further insights
- Accounting for storage processes in lakes, groundwater, snow/ice and reservoirs on watershed level to improve the WSI (especially relevant for monthly WSI) including inter-basin water transfer to improve water consumption locations (results from city-level analysis).

7.1.2 Specific tasks according to proposal

Task 2.1: Refinement of the distinction between surface and groundwater to smaller scale than national levels with global coverage (if step 1.6 is successful); introduce temporal differentiation for all WSI:

Groundwater

- Flow regime groundwater system (transmissivities, storages, infiltration)
- Vulnerabilities (combine with insights from Francesca's work)
- Address quality issues (groundwater and VEOLIA WII)
- Include more local data (higher spatial resolution, insights from master and bachelor theses)

Monthly data

- Instead of giving a temporal resolution strictly based on the calendar months moving averages could be considered including groundwater features and other storage mechanisms
- CTA monthly to be calculated
- Also surface and groundwater WSI can be adjusted on monthly level.

Task 2.2: Compare different kinds and types of Water Stress Indices and evaluate reduction of uncertainty by enhanced spatial resolution:

Adequacy of the different WSI

- Analyse use cases and useful combinations of the different WSI

Uncertainties

- Input data uncertainty (hydrological and use models)
- Conceptual uncertainty (model choice, WSI function)
- Sensitivities of choice (especially also regarding different types of WSI concepts)

Include drought events

- Adjust monthly WSI to drought risks

Task 2.3: Establish a future oriented WSI for scenarios in 2050 based on new publication of Pfister et al. (in press) and update these scenarios with the new data of Steps 1.1 – 1.2

Future aspect

- Analyse future scenarios for prospective WSI (Risk Assessment)

8 References

Alcamo, J., P. Döll, et al. (2003). "Development and testing of the WaterGAP 2 global model of water use and availability." Hydrological Sciences Journal 48(3): 317-337.

CEH Centre for Eclogy & Hydrology. "Information Gateway." Retrieved 5. March, 2012, from https://gateway.ceh.ac.uk/terraCatalog/Start.do.

Clark, D. B., L. M. Mercado, et al. (2011). "The Joint UK Land Environment Simulator (JULES), model description – Part 2: Carbon fluxes and vegetation dynamics." Geosci. Model Dev. 4(3): 701-722.

Cox, P. M., R. A. Betts, et al. (1999). "The impact of new land surface physics on the GCM simulation of climate and climate sensitivity." Climate Dynamics 15(3): 183-203.

Döll, P. and K. Fiedler (2008). "Global-scale modeling of groundwater recharge." Hydrol. Earth Syst. Sci. 12(3): 863-885.

Döll, P., H. Hoffmann-Dobrev, et al. (2011 (article in press)). "Impact of water withdrawals from groundwater and surface water on continental water storage variations." Journal of Geodynamics(0).

Döll, P., F. Kaspar, et al. (2003). "A global hydrological model for deriving water availability indicators: model tuning and validation." Journal of Hydrology 270(1-2): 105-134.

Döll, P., B. Lehner, et al. (2000). "Global modeling of groundwater recharge and surface runoff." EcoRegio 8: 73-80.

Döll, P., and Lehner, B. (2002): Validation of a new global 30-minute drainage direction map. Journal of Hydrology, 258(1-4), 214-231

Essery, R. L. H., M. J. Best, et al. (2003). "Explicit Representation of Subgrid Heterogeneity in a GCM Land Surface Scheme." Journal of Hydrometeorology 4(3): 530-543.

EU Sixth Framework Programme (2007-2011). "Integrated Project Water and Global Change (WATCH)." Retrieved Noveberm and December 2011, from http://www.eu-watch.org/about.

EU WATCH Sixth Framework Programme (2007-2011). "Global Modellling. Data Format." Retrieved 2. March, 2012, from http://www.eu-watch.org/watermip/data-format.

Flörke, M. and J. Alcamo (2004). European Outlook on Water Use. Final Report, Center for Environmental Systems Research. University of Kassel.

Flörke, M. and Eisner S. (2011). Technical Report No. 46. the development of global spatially detailed estimates of sectoral water requiremets, past, present and future, including discussion of the main uncertainties, risks and vulnerabilities of human water demand., Watch.

Gregory, D., R. N. B. Smith, et al. (1994). Canopy, surface and soil hydrology - Unified model documentation paper 25, Climate Research. Meteorological Office.

Haddeland, I., D. B. Clark, et al. (2011). "Multimodel Estimate of the Global Terrestrial Water Balance: Setup and First Results." Journal of Hydrometeorology 12(5): 869-884.

Hanasaki, N., T. Inuzuka, et al. (2010). "An estimation of global virtual water flow and sources of water withdrawal for major crops and livestock products using a global hydrological model." Journal of Hydrology 384(3-4): 232-244.

Hanasaki, N., S. Kanae, et al. (2006). "A reservoir operation scheme for global river routing models." Journal of Hydrology 327(1-2): 22-41.

Hanasaki, N., S. Kanae, et al. (2008a). "An integrated model for the assessment of global water resources – Part 1: Model description and input meteorological forcing." Hydrol. Earth Syst. Sci. 12(4): 1007-1025.

Hanasaki, N., S. Kanae, et al. (2008b). "An integrated model for the assessment of global water resources – Part 2: Applications and assessments." Hydrol. Earth Syst. Sci. 12(4): 1027-1037.

Lehner , B. and Döll, P. (2004): Development and validation of a global database of lakes, reservoirs and wetlands. Journal of Hydrology 296/1-4: 1-22.

Met Office and CEH Centre for Eclogy & Hydrology (2011). "Jules - Joint UK Land Environment Simulator." Retrieved 8th March, 2012, from http://www.jchmr.org/jules/.

Pfister, S., P. Bayer, et al. (2011). "Projected water consumption in future global agriculture: Scenarios and related impacts." Science of The Total Environment 409(20): 4206-4216.

Pfister, S., A. Koehler, et al. (2009). "Assessing the Environmental Impacts of Freshwater Consumption in LCA." Environmental Science & Technology 43(11): 4098-4104.

Rost S., G. D., Bondeau A., Lucht W., Rohwer J., Schaphoff S., (2008). "Agricultural green and blue water consumption and its influence on the global water system." Water Resource Research 44.

Siebert, S., J. Burke, et al. (2010). "Groundwater use for irrigation – a global inventory." Hydrol. Earth Syst. Sci. 14(10): 1863-1880.

van Beek, L. P. H. and M. F. P. Bierkens (2008). The Global Hydrological ModelPCR-GLOBWB: Conceptualization, Parameterization and Verification. Utrech, Netherlands, Department of Physical Geography. Utrech University.

van Beek, L. P. H., Y. Wada, et al. (2011). "Global monthly water stress: 1. Water balance and water availabilty." Water Resource Research 47.

Vörösmarty, C. J., C. Leveque, et al. (2005). Chapter 7: Fresh Water. Millennium Ecosystem Assessment. Volume 1: Conditions and Trends Working Group Report.

Voss, F., J. Alcamo, et al. (2008). Technical Report No. 1. First results form intercomparison of surface water availabilty modules. WATCH.

Voss, F., M. Flörke, et al. (2009). Technical Report No. 17. Preliminary spatially explicit estimates of past and present domestic water use., Watch.

Wada, Y., L. P. H. van Beek, et al. (2010). "Global depletion of groundwater resources." Geophys. Res. Lett. 37(20): L20402.

Weedon, G. P. (2011). Technical Report No. 37. Creation of the WATCH 20th century ensemble product. WATCH.

9 Appendix

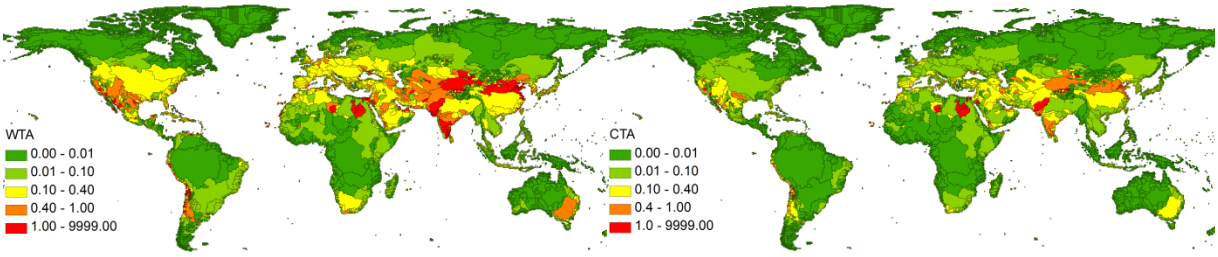

Figure 48: Withdrawal to Availability ratio WTA (left) and Consumption to Availability ratio CTA (right), calculated based on the WATCH data

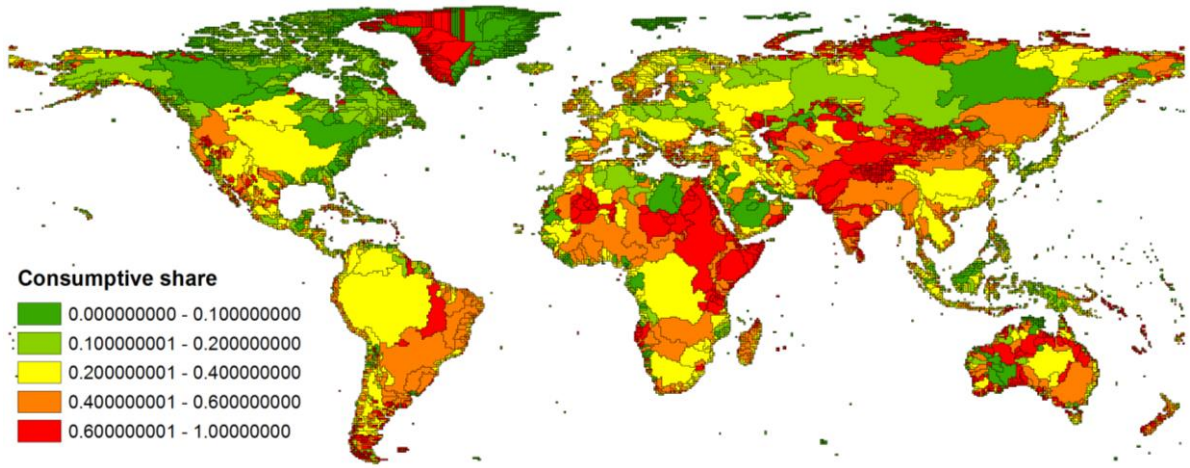

Figure 49: Consumption to withdrawal ratio calculated based on the total consumption and withdrawal data provided by WATCH

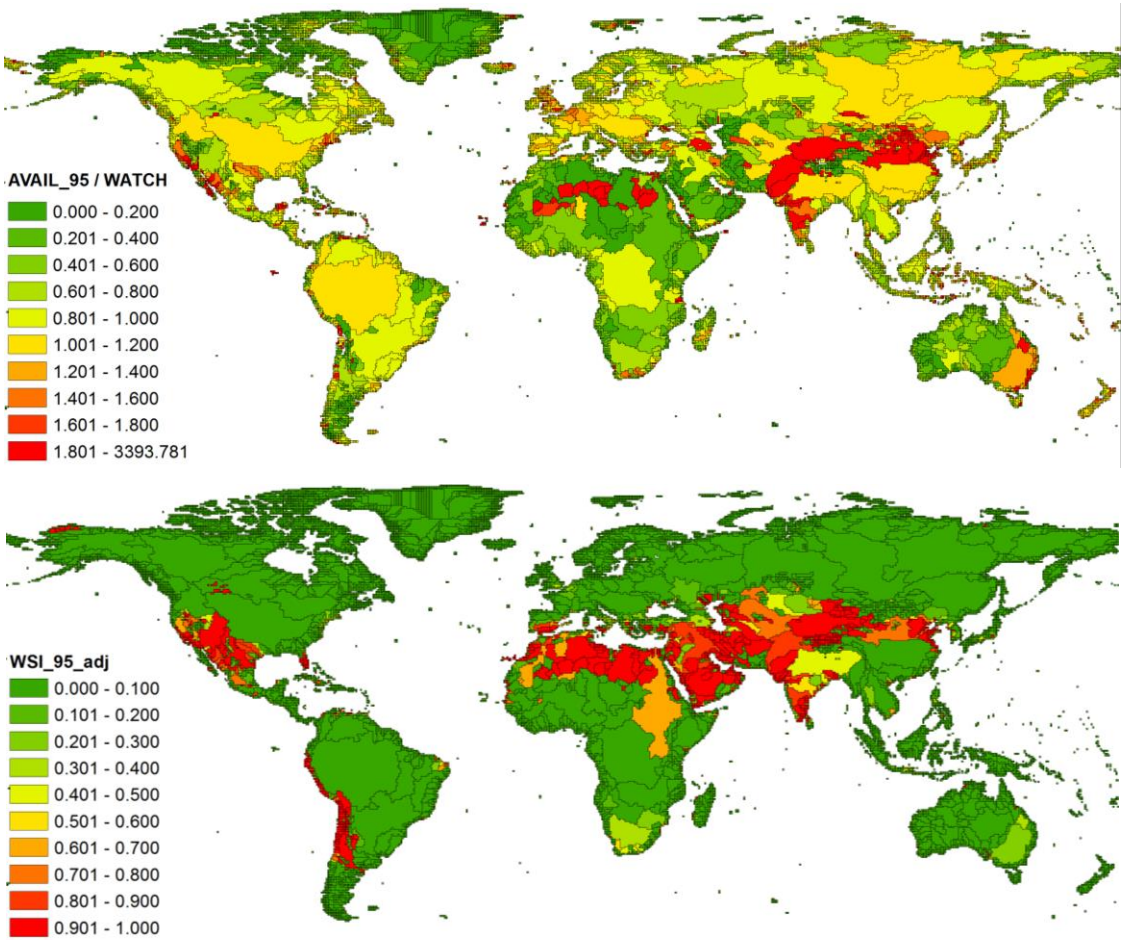

Figure 50: The availability by Alcamo is corrected by adding the withdrawal to the actual discharge (top) and corresponding WSI (bottom)

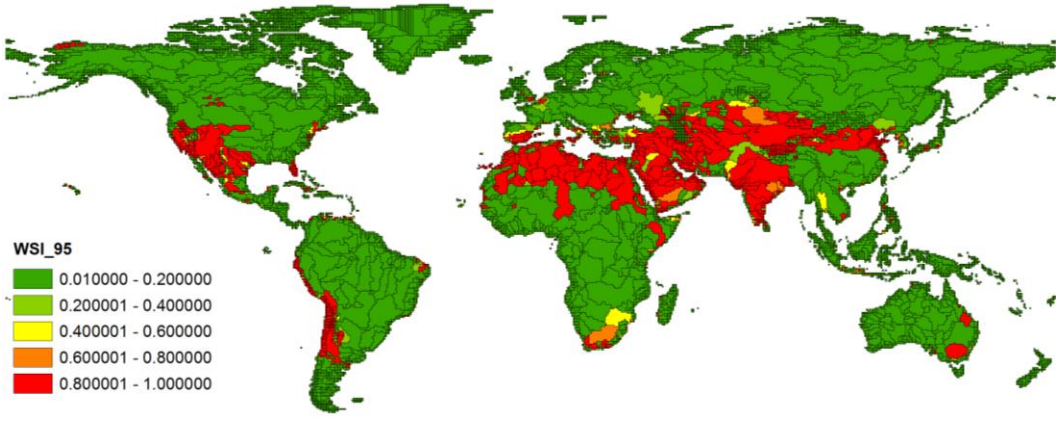

Figure 51: Withdrawal based Water Stress Index [m^3/m^3] calculated based on WaterGAP model data provided by Alcamo for the watershed structure by Floecke et al.

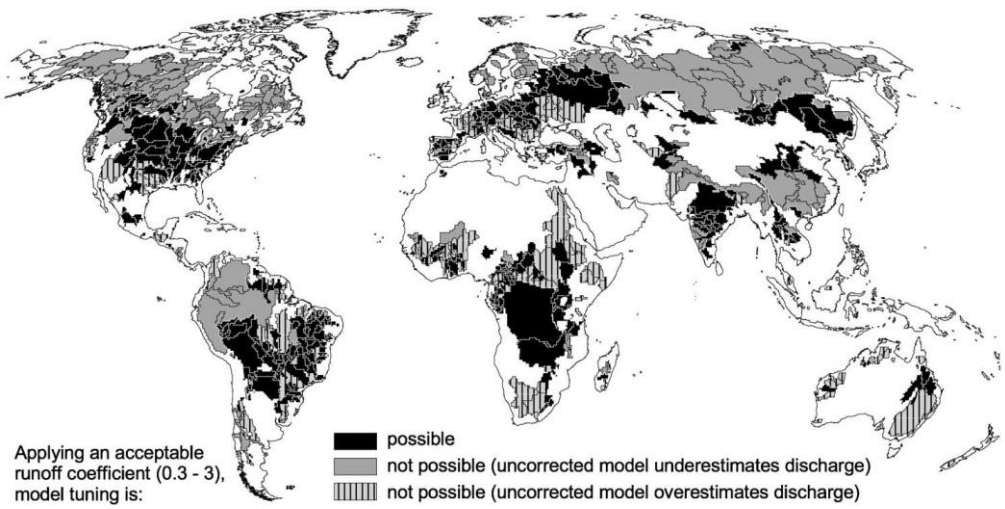

Figure 52: Tuning watersheds in which WHGM can be calibrated by adjusting the runoff coefficient within physically plausible limits.(Döll et al. 2002)